STUDIES ON THE THERMAL BEHAVIOUR OF PARTICLE FILLED EPOXY USED IN MICROELECTRONIC DEVICES

A THESIS SUBMITTED TO
THE GRADUATE SCHOOL OF NATURAL AND APPLIED SCIENCES
OF
MIDDLE EAST TECHNICAL UNIVERSITY

BY

ESİN AKÇA

IN PARTIAL FULFILLMENT OF THE REQUIREMENTS
FOR
THE DEGREE OF DOCTOR OF PHILOSOPHY
IN
METALLURGICAL AND MATERIALS ENGINEERING

FEBRUARY 2026

Approval of the thesis:

STUDIES ON THE THERMAL BEHAVIOUR OF PARTICLE FILLED EPOXY USED IN MICROELECTRONIC DEVICES

submitted by **ESİN AKÇA** in partial fulfillment of the requirements for the degree of **Doctor of Philosophy in Metallurgical and Materials Engineering, Middle East Technical University** by,

Prof. Dr. Naci Emre Altun
Dean, **Graduate School of Natural and Applied Sciences** _____

Prof. Dr. M. Kadri Aydınol
Head of the Department, **Metallurgical and Materials Eng. Dept., METU** _____

Prof. Dr. Cevdet Kaynak
Supervisor, **Metallurgical and Materials Eng. Dept., METU** _____

Examining Committee Members:

Prof. Dr. Necati Özkan
Polymer Science and Technology, METU _____

Prof. Dr. Cevdet Kaynak
Metallurgical and Materials Eng., METU _____

Prof. Dr. Bora Maviş
Mechanical Engineering Dept., Hacettepe University _____

Assoc. Prof. Dr. Batur Ercan
Metallurgical and Materials Eng., METU _____

Assist. Prof. Dr. Salih Ertan
Chemical Engineering Dept., Atılım University _____

Date: 27.02.2026

I hereby declare that all information in this document has been obtained and presented in accordance with academic rules and ethical conduct. I also declare that, as required by these rules and conduct, I have fully cited and referenced all material and results that are not original to this work.

Name, Last name : Esin Akça
Signature :

ABSTRACT

STUDIES ON THE THERMAL BEHAVIOUR OF PARTICLE FILLED EPOXY USED IN MICROELECTRONIC DEVICES

Akça, Esin
Ph.D., Department of Metallurgical and Materials Engineering
Supervisor: Prof. Dr. Cevdet Kaynak

February 2026, 100 pages

The main purpose of this study was to investigate effects of 10, 20, 40 wt% micron-sized particles (aluminum nitride, aluminum oxide, silicon nitride, silicon oxide) on the thermal performance of epoxy resin used in microelectronic devices. Specimens were produced via solution mixing technique followed by molding and curing. Although there were slight differences between each particle used, various thermal analyses conducted revealed that increasing the amount of all particles improved the thermal performance of the epoxy resin more significantly.

The most significant property influencing thermal performance of these devices would be Thermal Conductivity (λ). Because heat development during operation should be released via heat diffusion which requires certain level of λ . In this study, use of 40 wt% particles increased the Thermal Conductivity (λ) of neat epoxy (0.15 W/m. K) more than 3 times.

Another significant problem during operation of these devices would be formation of “thermal strain mismatch” due to the different values of Thermal Expansion Coefficient (α) of each material used in the device that might lead to loss of

dimensional stability and malfunctioning. In this study, use of 40 wt.% particles decreased the thermal expansion coefficient of epoxy ($49x10^{-6}$/K) down to $28x10^{-6}$/K, i.e. a decrease of -43%.

Thermal performance also depends on the Glass Transition Temperature (T_g) values. In this study, use of 40 wt% particles increased T_g of neat epoxy (51°C) to 68°C, i.e. an increase of 17°C. Similarly, use of 40 wt% particles increased the Thermal Degradation Temperature (T_d) of neat epoxy (324°C) to 356°C; i.e. an increase of 32°C.

Moreover, it was also revealed that, there was no decrease in the lap shear adhesion strength of the neat epoxy resin after the incorporation of all particles. Additionally, these particles also increased mechanical rigidity of neat epoxy in terms of Storage Modulus at 25°C and 50°C.

Keywords: Epoxy resin; aluminum nitride; aluminum oxide; silicon nitride; silicon oxide; thermal behaviour; microelectronic devices.

ÖZ

MİKROELEKTRONİK CİHAZLARDA KULLANILAN PARÇACIK DOLGULU EPOKSİNİN ISIL DAVRANIŞI ÜZERİNE ÇALIŞMALAR

Akça, Esin
Doktora, Metalurji ve Malzeme Mühendisliği Bölümü
Tez Yöneticisi: Prof. Dr. Cevdet Kaynak

Şubat 2026, 100 sayfa

Bu çalışmanın temel amacı, mikroelektronik cihazlarda kullanılan epoksi reçinenin ısıl performansı üzerine %10, %20 ve %40 ağırlıkça mikron boyutlu parçacıkların (alüminyum nitrür, alüminyum oksit, silikon nitrür, silikon oksit) etkilerini incelemektir. Numuneler, çözelti karıştırma tekniği ile hazırlanmış, ardından kalıplama ve kürleme işlemleri uygulanmıştır. Her bir parçacık türü arasında küçük farklılıklar bulunmakla birlikte, gerçekleştirilen çeşitli ısıl analizler, tüm parçacıklar için dolgu miktarının artmasının epoksi reçinenin ısıl performansını belirgin şekilde iyileştirdiğini ortaya koymuştur.

Bu tür cihazların ısıl performansını etkileyen en önemli özelliklerden biri ısı iletkenliği (λ)'dir. Çalışma sırasında oluşan ısının, yeterli bir ısı iletkenliği seviyesini gerektiren ısı yayılımı yoluyla ortamdan uzaklaştırılması gerekmektedir. Bu çalışmada, %40 ağırlıkça dolgu kullanımı, saf epoksinin ısı iletkenliği değerini (0,15 W/m·K) üç kattan fazla artırmıştır.

Cihazların çalışma sürecinde karşılaşılan bir diğer önemli sorun ise, cihazda kullanılan farklı malzemelerin ısıl genleşme katsayılarının (α) farklı olmasından kaynaklanan ve boyutsal kararsızlık nedeniyle fonksiyon kaybına yol açabilen "ısıl gerinim uyumsuzluğu"nun oluşmasıdır. Bu çalışmada, %40 ağırlıkça dolgu kullanımı ile epoksinin ısıl genleşme katsayısı 49×10^{-6} /K değerinden 28×10^{-6} /K değerine düşmüş olup, bu durum yaklaşık %43'lük bir azalmaya karşılık gelmektedir.

Isıl performans aynı zamanda camsı geçiş sıcaklığı (T_g) değerlerine de bağlıdır. Bu çalışmada, %40 ağırlıkça dolgu kullanımı, saf epoksinin T_g değerini 51°C'den 68°C'ye yükseltmiş, yani 17°C'lik bir artış sağlamıştır. Benzer şekilde, %40 ağırlıkça dolgu kullanımı saf epoksinin ısıl bozunma sıcaklığını (T_d) 324°C'den 356°C'ye çıkarmış, bu da 32°C'lik bir artışa karşılık gelmektedir.

Ayrıca, tüm parçacıkların ilave edilmesinden sonra saf epoksi reçinenin lap-shear yapışma dayanımında herhangi bir azalma olmadığı da ortaya konmuştur. Buna ek olarak, bu parçacıklar 25°C ve 50°C'de ölçülen Depolama Modül değerleri açısından saf epoksinin mekanik rijitliğini de artırmıştır.

Anahtar Kelimeler: Epoksi reçine; alüminyum nitrür; alüminyum oksit; silikon nitrür; silikon oksit; ısıl davranış; mikroelektronik cihazlar.

To My Family

ACKNOWLEDGEMENTS

First and foremost, I would like to express my sincere gratitude to my advisor, Prof. Dr. Cevdet Kaynak, for his invaluable guidance, support and encouragement throughout the course of this thesis.

I am thankful to the members of my thesis examining committee, Prof. Dr. Necati Özkan and Assoc. Prof. Dr. Batur Ercan, for their valuable feedback and constructive suggestions.

I would also like to extend my thanks to the Department of Micro Electronics Design at ASELSAN for providing access to the facilities and resources necessary for this work. The support and opportunities ASELSAN offered have played a vital role in completing this thesis. In particular, I would like to extend my deepest gratitude to my colleagues at Post-Process Team for their valuable discussions, cooperation, and support during both the experimental and writing phases of this study. Their contributions and shared knowledge were instrumental in overcoming challenges encountered throughout the research process.

Special thanks are extended to the technical staff at National Nanotechnology Research Center (UNAM) for their assistance with the calibration of the equipment.

I am also thankful to Dr. Jane Frommer who was the first person who supports me for this study. My conversations with her at IBM Almaden Research Center have planted the seeds of this thesis.

Finally, I am deeply grateful to my family for their unwavering support, understanding, and encouragement throughout this academic journey. I would like to thank my spouse and my child for their love, patience, and constant motivation.

TABLE OF CONTENTS

ABSTRACT v

ÖZ vii

ACKNOWLEDGEMENTS x

TABLE OF CONTENTS xi

LIST OF TABLES xiv

LIST OF FIGURES xv

LIST OF ABBREVIATIONS xvii

LIST OF SYMBOLS xviii

CHAPTERS

1 INTRODUCTION 1

1.1 Epoxies Used in Electronic Devices 1

1.2 Introduction to Thermal Properties of Epoxy 10

1.2.1 Isothermal Curing Behaviour 10

1.2.2 Thermal Conductivity 12

1.2.3 Thermal Expansion Coefficient 12

1.2.4 Glass Transition Temperature 13

1.2.5 Thermal Degradation Temperature 14

1.2.6 Adhesion Strength 15

1.3 Previous Studies on the Effects of Nitride and Oxide Particles 17

1.4 Aim of This Thesis 25

2 EXPERIMENTAL WORK 29

2.1 Epoxy Resin System and Oxide / Nitride Particles Used 29

2.2 Dynamic Light Scattering (DLS) Analysis 32
2.3 Scanning Electron Microscopy (SEM) Analysis 32
2.4 Production of the Particle Filled Epoxy Samples 34
2.5 Differential Scanning Calorimetry (DSC) Analysis 38
2.6 Thermal Conductivity Analysis 38
2.7 Dilatometry Analysis 39
2.8 Dynamic Mechanical Analysis (DMA) 40
2.9 Thermogravimetric Analysis (TGA) 41
2.10 Lap Shear Adhesion Tests 42
3 RESULTS AND DISCUSSION 45
3.1 Size Range and Dispersion of the Oxide and Nitride Particles in Epoxy Matrix ….. 45
3.2 Effects of Particles on the Isothermal Curing Behaviour 55
3.3 Effects of Particles on the Thermal Conductivity 63
3.4 Effects of Particles on the Thermal Expansion Coefficient 65
3.5 Effects of Particles on the λ/α Ratio 67
3.6 Effects of Particles on the Glass Transition Temperature 68
3.7 Effects of Particles on the Thermal Degradation Temperature 73
3.8 Effects of Particles on the Adhesion Strength 77
3.9 Effects of Particles on the Storage Modulus 80
3.10 Relevance of the Results to Microelectronic Applications 84
4 CONCLUSIONS AND FUTURE RECOMMENDATIONS 87
4.1 Conclusions 87
4.2 Future Recommendations 89

REFERENCES 91
CURRICULUM VITAE 99

LIST OF TABLES

TABLES

Table 3.1. Effects of Particles on the values of $t_{50\%}$, $t_{75\%}$ and $t_{100\%}$ (Time required for 50%, 75% and 100% curing Conversion) 61
Table 3.2. Effects of Particles on the values of λ, α, λ/α, T_g and T_d of Epoxy. 77
Table 3.3. Effects of Particles on the values of Storage Modulus (E') of Epoxy at 25°C and 50°C. 82

LIST OF FIGURES

FIGURES

Figure 1.1. The chemical structure of DGEBA. 1
Figure 1.2. Different applications where epoxy based polymeric materials are used in microelectronics [7,8]. 7
Figure 2.1. Materials used in this study; (a) epoxy resin and curing agent, (b) AlN, (c) Al_2O_3, (d) Si_3N_4 and (e) SiO_2 particles. 31
Figure 2.2. DLS equipment used in this study. 32
Figure 2.3. Sampling (a), gold sputtering (b) and main SEM equipment (c) used in this study. 33
Figure 2.4. Two main stages used for the production of liquid samples and solid specimens. 35
Figure 2.5. Equipment used in stage 1; (a) mixing of fillers into the curing agent, (b) ultrasonic bath, (c) adding epoxy resin into the mixture, (d) magnetic stirrer, (e,f) sample holder and speed mixer equipment used in this study. 36
Figure 2.6. Equipment used in stage 2 for liquid samples; (a) mixing of epoxy resin and curing agent and (b) filling DSC pans by using syringe needle. 37
Figure 2.7. Equipment used in stage 2 for solid specimens; (a) master molds to produce molds, (b) mold in vertical holder, (c) curing furnace and (d) solid specimens after curing in molds. 37
Figure 2.8. DSC equipment used in this study. 38
Figure 2.9. Thermal conductivity measurement equipment used in this study. 39
Figure 2.10. Dilatometry equipment used in this study. 40
Figure 2.11. DMA equipment used in this study. 41
Figure 2.12. TGA equipment used in this study. 42

Figure 2.13. (a) Schematic showing the dimensions of lap shear adhesion test specimens, (b) Test specimens attached to the fixture (c) Universal Testing System used in this study. 43
Figure 3.1. SEM images showing size range and morphology of the particles. 47
Figure 3.2. Size distribution of the particles determined by DLS analyses. 49
Figure 3.3. SEM images showing dispersion of particles in the epoxy matrix. 51
Figure 3.4. Effects of particles on the isothermal Heat Flow versus Time curves of epoxy. 56
Figure 3.5. Effects of particles on the curing Conversion versus Time curves of epoxy. 58
Figure 3.6. Effects of particle type and content on the curing Conversion versus Time curves of epoxy..... 60
Figure 3.7. Effects of Particles on the Thermal Conductivity of Epoxy. 64
Figure 3.8. Effects of Particles on the Thermal Expansion Coefficient of Epoxy. . 66
Figure 3.9. Effects of Particles on the *tan δ* curves of Epoxy determined by DMA. 69
Figure 3.10. Effects of Particles on the Glass Transition Temperature of Epoxy. .. 71
Figure 3.11. Effects of Particles on the Thermogravimetric (TG), and in the insets, Derivative Thermogravimetric (DTG) Curves of Epoxy. 74
Figure 3.12. Effects of Particles on the Thermal Degradation Temperature of Epoxy. 76
Figure 3.13. Effects of Particles on the Lap Shear Adhesion Strength of Epoxy. .. 79
Figure 3.14. Failure modes of Lap Shear Test. 79
Figure 3.15. Examples of the “Mixed” Failure Mode observed after Lap Shear Tests. 80
Figure 3.16. Effects of Particles on the Storage Modulus of Epoxy. 83

LIST OF ABBREVIATIONS

ABBREVIATIONS

AlN	:	Aluminum Nitride
Al_2O_3	:	Aluminum Oxide
BPA	:	Bisphenol A
DGEBA	:	Diglycidyl Ether of Bisphenol A
DLS	:	Dynamic Light Scattering
DMA	:	Dynamic Mechanical Analysis
DSC	:	Differential Scanning Calorimetry
EP	:	Epoxy
MEMS	:	Micro Electromechanical Systems
PSD	:	Particle Size Distribution
SEM	:	Scanning Electron Microscopy
Si_3N_4	:	Silicon Nitride
SiO_2	:	Silicon Oxide
TGA	:	Thermogravimetric Analysis
vol%	:	Volume Percent
wt%	:	Weight Percent

LIST OF SYMBOLS

SYMBOLS

°C	:	Degree Celsius
E’	:	Storage Modulus (MPa)
E”	:	Loss Modulus (MPa)
h	:	Hour
mg	:	milligram
min	:	Minute
ml	:	Milliliter
mm	:	Millimeters
mm^2	:	Millimeters square
rpm	:	Revolutions per minute
T	:	Temperature
$Tan\ \delta$	:	Loss factor
T_g	:	Glass Transition Temperature
T_d	:	Decomposition Temperature
α	:	Thermal Expansion Coefficient
λ	:	Thermal Conductivity

CHAPTER 1

INTRODUCTION

Epoxy resins are widely used in electronic applications due to their high chemical resistance, excellent mechanical properties, good adhesion to different types of materials, low shrinkage, ease of viscosity control, low vapor pressure etc. Although epoxy resins have many advantages, conventional formulations mostly fail to meet the stringent requirements, so they are filled with fillers. As filler size and loading have huge impact on the properties, the use of filler particles is considered as one of the most promising solutions.

1.1 Epoxies Used in Electronic Devices

Epoxy resins represent an important class of thermosetting polymers widely utilized in various industrial and technological fields due to their excellent mechanical, chemical and electrical properties. Chemically, epoxy resins are characterized by the presence of reactive epoxide groups in their molecular structure. The most common type of epoxy resin is based on the reaction between bisphenol A (BPA) and epichlorohydrin, forming diglycidyl ether of bisphenol A (DGEBA), which has the general chemical formula of $C_{21}H_{24}O_4$ (Figure 1.1).

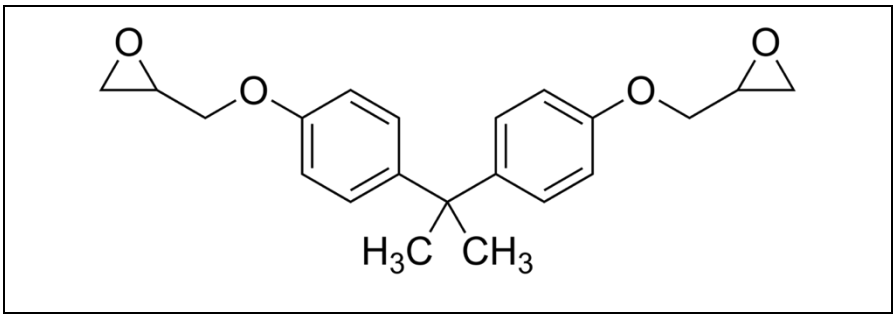

Figure 1.1. The chemical structure of DGEBA.

The key functional group in epoxy resins is the epoxide ring (-C-O-C-), which can undergo ring-opening reactions with various curing agents such as amines, anhydrides, or acids, resulting in a highly crosslinked and rigid polymer network [1].

Epoxy materials are preferred for their outstanding adhesion, chemical resistance, thermal stability, and dimensional stability. These properties make them suitable for a wide range of applications, including coatings, adhesives, structural composites, and tooling. In the electronics industry, epoxy resins play a crucial role in several areas (Figure 1.2):

- **Die Bonding Adhesives**

Die bonding adhesives are used to bond semiconductor chips to substrates, lead frames, or package bases. Epoxy resins provide both mechanical fixation and thermal conduction pathways, critical for dissipating heat generated during device operation. Die attach epoxies are designed to have high bond strength and thermal stability, ensuring device reliability under thermal cycling and high operational temperatures.

In MEMS device packaging, epoxy adhesives are employed for structural bonding of microscale components. These adhesives must exhibit high mechanical strength, low modulus (in some cases), and compatibility with microfabrication processes. Epoxies enable precise alignment and bonding at low processing temperatures, making them suitable for delicate MEMS structures [2].

- **Underfill**

Epoxy underfills are extensively used in flip chip and ball grid array (BGA) packaging to mechanically reinforce solder joints. These materials fill the gap between the die and substrate, mitigating stress from thermal expansion coefficient

mismatches. This encapsulation method enhances mechanical stability, prevents solder fatigue, and improves thermal cycling reliability, which is essential for high-performance electronic assemblies [3].

Beyond mechanical reinforcement, underfill materials significantly influence the thermal and viscoelastic behaviour of flip chip and ball grid array assemblies. The cured underfill redistributes thermomechanical stresses more uniformly across the solder joints, thereby reducing localized stress concentrations that can accelerate crack initiation and propagation. Furthermore, the incorporation of thermally conductive yet electrically insulating fillers enables underfills to contribute to heat dissipation without compromising electrical performance. Optimizing key material parameters such as glass transition temperature, elastic modulus, and thermal conductivity is therefore critical to achieving a balance between stress relief and structural integrity, ultimately enhancing the long-term reliability of advanced electronic packages subjected to repeated thermal cycling and harsh operating environments.

- **Glob Top Encapsulation**

Glob top encapsulation involves dispensing epoxy resin directly over wire-bonded semiconductor devices, forming a protective encapsulant. This method is employed to secure delicate interconnects from mechanical shocks, moisture ingress, and corrosive environments. The epoxy formulation is optimized for low shrinkage, minimal outgassing, and thermal stability to maintain package integrity and ensure long-term device functionality [4].

In addition to environmental protection, glob top encapsulation plays a critical role in stress redistribution within wire-bonded assemblies. The cured epoxy layer provides mechanical damping that reduces stress concentrations at wire bond heels

and bond pads during thermal cycling and mechanical loading. Careful control of material properties such as elastic modulus, thermal expansion coefficient and glass transition temperature is essential to prevent excessive stress transfer to the interconnects. Furthermore, filled epoxy systems are often employed to tailor rheological behaviour during dispensing and to enhance thermal performance after curing. These design considerations enable glob top encapsulants to maintain structural integrity and electrical reliability in miniaturized electronic packages operating under demanding environmental conditions.

- **Conformal Coating**

Epoxy based conformal coatings are applied as thin, uniform layers onto printed circuit boards and electronic assemblies to provide protection against environmental factors such as moisture, chemicals, and ionic contaminants. These coatings act as dielectric barriers, preventing electrical leakage and corrosion while enhancing mechanical stability. Their high glass transition temperature and chemical inertness make them suitable for demanding operating conditions.

In addition to their protective function, conformal coatings contribute to the long-term reliability of electronic assemblies by stabilizing surface insulation resistance under humid and contaminated environments. The uniform coating layer suppresses electrochemical migration and dendritic growth, which are common failure mechanisms in high-density circuit layouts [5]. Moreover, the controlled thickness and cured network structure of epoxy coatings allow them to accommodate minor substrate deformation without cracking or delamination. Optimization of key parameters such as crosslink density, adhesion to metallic and polymeric surfaces, and thermal stability is therefore essential to ensure consistent electrical performance and mechanical integrity throughout extended service life and thermal cycling exposure.

- **Optical Encapsulation**

Optically clear epoxy resins are employed for the encapsulation of optoelectronic components, including LEDs, photodiodes, and fiber-optic assemblies. These materials provide both mechanical protection and optical transparency, ensuring minimal light attenuation. Low-stress formulations are often selected to avoid optical distortions and to maintain precise alignment of optical pathways.

Beyond optical transparency, the long-term performance of optically clear epoxy resins is strongly governed by their photothermal and environmental stability. Exposure to elevated temperatures, ultraviolet radiation, and moisture can induce yellowing, refractive index changes, or microcrack formation, which adversely affect optical efficiency and signal integrity. Consequently, these epoxy systems are carefully formulated to exhibit low moisture absorption, stable refractive index, and high resistance to photodegradation. In addition, precise control of curing kinetics and residual stresses is essential to minimize birefringence and optical path distortion, thereby ensuring consistent optical output and reliable operation of optoelectronic devices over extended service lifetimes [4].

- **Potting and Sealing**

Epoxy potting compounds are used to encapsulate entire electronic modules for protection against environmental stresses such as humidity, vibration, chemical exposure, and thermal shock. These materials form a rigid or semi-rigid encapsulant that shields sensitive components from mechanical and environmental damage while also providing electrical insulation. High thermal stability and low water permeability are critical properties for potting applications in automotive and aerospace systems [6].

In addition to environmental protection, epoxy potting compounds significantly influence the thermomechanical behaviour and reliability of fully encapsulated electronic modules. The cured encapsulant alters heat dissipation pathways and stress distribution within the assembly, making the control of elastic modulus, thermal expansion coefficient, and thermal conductivity essential for minimizing internal stress accumulation. Filler modified epoxy systems are frequently employed to tailor these properties, enabling improved vibration damping and enhanced resistance to thermal shock. Such material optimization is particularly critical in different applications, where electronic modules are routinely subjected to wide temperature fluctuations, mechanical loads, and long service lifetimes under harsh operating conditions.

Overall, the versatility of epoxy systems in electronic packaging arises from their ability to be precisely tailored to meet application-specific mechanical, thermal, electrical, and environmental requirements. Through formulation control, including resin chemistry, curing behaviour, and filler incorporation, epoxy materials can simultaneously provide structural integrity, stress mitigation, thermal management, and long-term reliability. Whether employed as die attach adhesives, underfills, encapsulants, coatings, or potting compounds, epoxies serve as multifunctional materials that directly influence device performance and service lifetime. As electronic assemblies continue to evolve toward higher power densities, increased miniaturization, and harsher operating environments, the optimization of epoxy-based materials remains a critical aspect of advanced electronic and microelectronic system design.

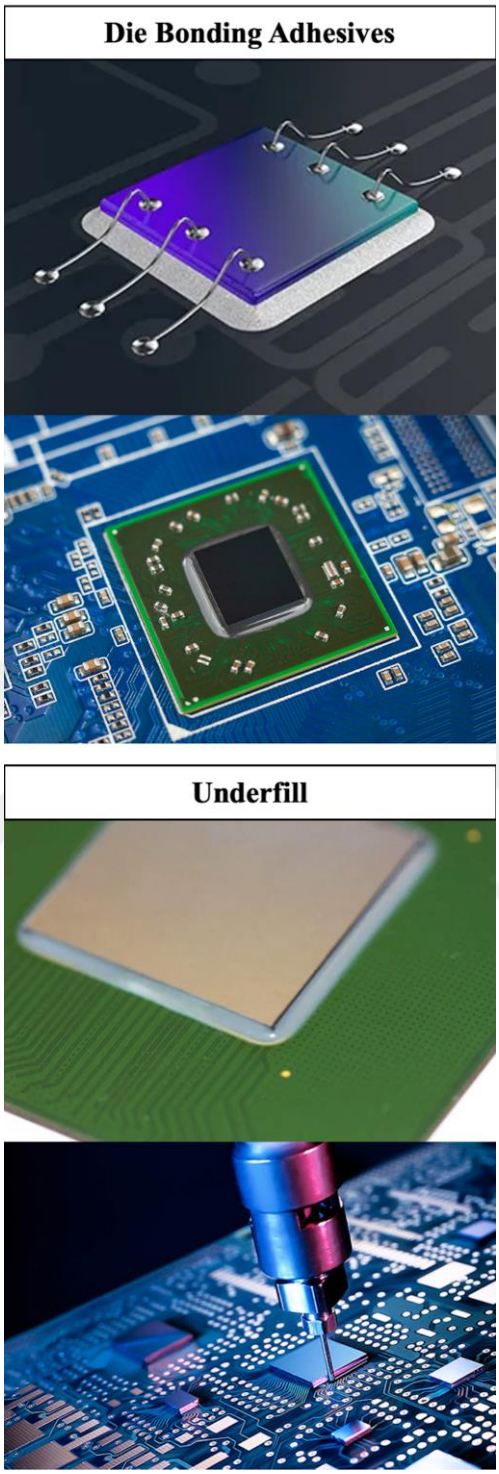

Figure 1.2. Different applications where epoxy based polymeric materials are used in microelectronics [7,8].

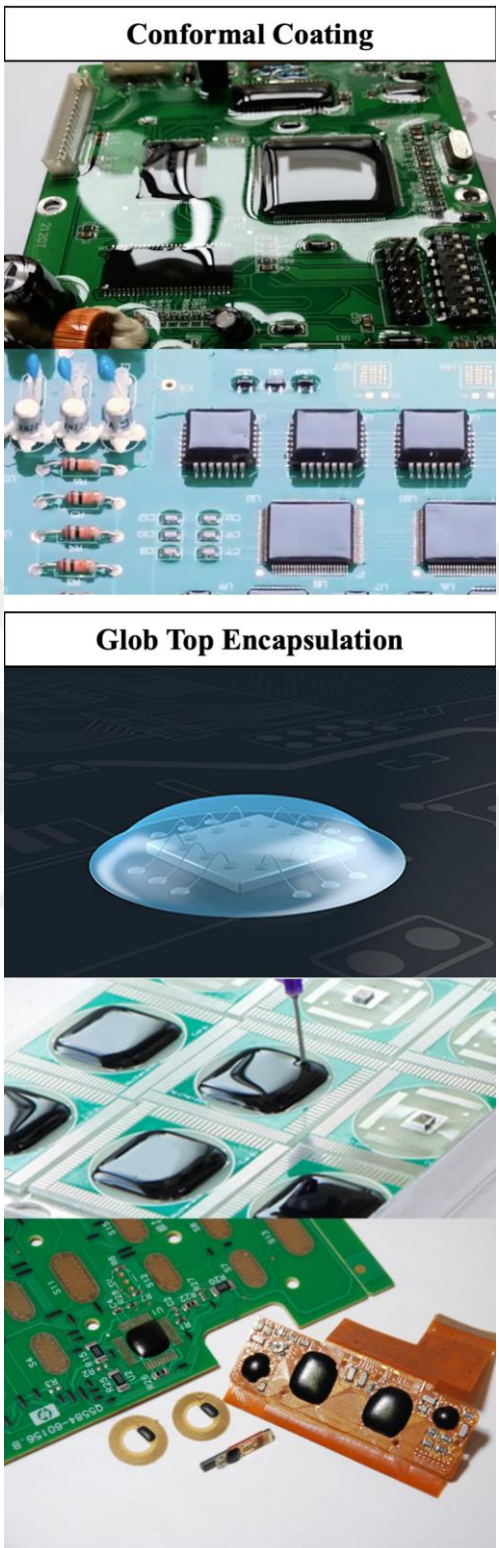

Figure 1.2. Continued [8,9].



Figure 1.2. Continued [10,11].

1.2 Introduction to Thermal Properties of Epoxy

1.2.1 Isothermal Curing Behaviour

Isothermal curing behaviour describes the evolution of a thermosetting polymer system when the curing reaction proceeds at a constant temperature. Under isothermal conditions, the thermal history is fixed, enabling precise evaluation of reaction kinetics, network formation, and diffusion-controlled limitations independent of continuously varying temperature effects. This approach is particularly advantageous for understanding structure–property relationships in epoxy-based materials.

During isothermal curing, low-molecular-weight oligomers progressively transform into a three-dimensional crosslinked network through curing reactions. The extent of reaction is quantified by the degree of cure, defined as the fraction of reacted functional groups relative to the total available reactive groups. The cure rate depends primarily on the reaction mechanism and molecular mobility at the selected curing temperature.

For many epoxy–amine systems, the reaction follows an autocatalytic mechanism in which hydroxyl groups generated during ring-opening reactions accelerate further curing. The kinetic behaviour is commonly represented by semi-empirical rate models such as nth-order or autocatalytic expressions. Under strictly isothermal conditions, the temperature-dependent rate constant remains constant throughout the experiment, and therefore the cure progression becomes solely time-dependent.

Differential Scanning Calorimetry (DSC) is a thermoanalytical technique used to measure the difference in heat flow between a sample and a reference as a function of temperature or time under a controlled heating or cooling program. In isothermal DSC analysis, the curing reaction is monitored through the exothermic heat flow signal recorded as a function of time. The measured heat flow rate is directly proportional to the instantaneous reaction rate. Therefore, the reaction rate can be derived from the normalized heat flow signal [12,13].

The degree of conversion at a given time is obtained by integrating the exothermic heat flow with respect to time and normalizing it by the total reaction enthalpy. In other words, the cumulative heat released up to a specific time represents the fraction of the total curing reaction that has occurred.

The incorporation of fillers significantly influences the isothermal curing behaviour of epoxy systems. Under isothermal conditions, the presence of rigid inorganic particles modifies heat transfer within the reacting medium and may introduce interfacial interactions between filler surfaces and the epoxy matrix. At low to moderate loadings, certain fillers can promote autocatalytic effects by facilitating additional hydrogen bonding or catalytic interactions, leading to a slight acceleration in the early-stage reaction rate. Conversely, high filler loadings generally reduce molecular mobility due to increased viscosity and restricted chain motion, thereby delaying gelation time and lowering the maximum attainable degree of cure under diffusion-controlled regimes. The overall effect of particulate fillers on isothermal curing kinetics strongly depends on filler type, surface chemistry, and loading fraction.

1.2.2 Thermal Conductivity

Thermal conductivity is a measure of a material's ability to conduct heat and is a key performance parameter for polymers used in microelectronic applications. In epoxy resins, thermal conductivity is inherently low due to the amorphous molecular structure and phonon scattering within the polymer matrix.

Thermal conductivity measurements are typically performed using steady-state or transient techniques, which evaluate heat flow through a specimen under a controlled temperature gradient. The measured thermal conductivity reflects the efficiency of heat dissipation from heat-generating components.

The addition of thermally conductive fillers such as nitride and oxide particles significantly enhances the thermal conductivity of epoxy composites by forming heat conduction pathways. Factors such as filler type, particle size, loading level and dispersion quality strongly influence the resulting thermal performance. Improved thermal conductivity is essential for reducing operating temperatures and improving the reliability of microelectronic devices.

1.2.3 Thermal Expansion Coefficient

Thermal expansion coefficient (α) describes the dimensional change of a material in response to temperature variation and is a critical parameter for polymeric materials used in microelectronic packaging. α is commonly measured using a dilatometer, which records the change in length of a specimen as a function of temperature.

For epoxy systems, thermal expansion coefficient behaviour is typically divided into two regions: below and above the glass transition temperature (T_g). Below T_g, the polymer exhibits a relatively low thermal expansion coefficient due to restricted molecular motion. Above T_g, increased chain mobility results in a significantly higher thermal expansion coefficient.

In filled epoxy composites, the incorporation of inorganic fillers reduces the overall thermal expansion of the material, thereby minimizing thermal strain mismatch with substrates such as silicon or ceramics. Accurate measurement of thermal expansion coefficient is crucial for ensuring dimensional stability and reliability in electronic and optoelectronic applications.

1.2.4 Glass Transition Temperature

Dynamic Mechanical Analysis (DMA) is used to characterize the viscoelastic behaviour of polymers by applying a small oscillatory deformation and measuring the material response as a function of temperature, frequency, or time. One of the most important parameters obtained from DMA is the loss factor (*tan δ*) defined as the ratio of the loss modulus (E″) to the storage modulus (E′).

Tan δ represents the damping behaviour of the material and is associated with energy dissipation due to molecular motion. In epoxy systems, the peak in the *tan δ* curve corresponds to the glass transition temperature, where segmental motion of polymer chains becomes dominant. Compared to DSC, DMA-derived T_g values are often higher as DMA probes mechanical relaxation rather than thermal transitions.

The magnitude and width of the *tan δ* peak provide information about molecular homogeneity, crosslink density and filler dispersion. A lower *tan δ* value generally indicates a stiffer, more elastic material, while higher values suggest increased viscous behaviour. DMA and *tan δ* analysis are therefore essential for evaluating mechanical performance and thermo-mechanical stability of materials [12,13].

1.2.5 Thermal Degradation Temperature

Thermogravimetric Analysis (TGA) is a thermal analysis technique that measures the mass change of a material as a function of temperature or time under a controlled atmosphere. TGA is commonly used to assess the thermal stability, decomposition behaviour, and compositional characteristics of polymeric materials.

For epoxy systems, TGA provides insight into degradation temperatures, thermal resistance, and filler effects on stability. The decomposition temperature (T_d) indicates the temperature at which significant thermal degradation begins, while the maximum degradation rate temperature corresponds to the peak of the derivative thermogravimetric (DTG) curve. Multi-step weight loss behaviour may be observed, reflecting different degradation mechanisms such as resin decomposition, char formation, or filler–matrix interactions.

At low temperatures, the TGA curve exhibits a nearly horizontal baseline, indicating negligible mass loss. In this region, the epoxy material remains thermally stable, and no significant physical or chemical degradation occurs. This region confirms the absence of volatile components and indicates that the material does not undergo premature thermal degradation before the onset of decomposition.

The epoxy undergoes mass loss due to the breakdown of the polymer backbone and the scission of crosslinked structures. The temperature corresponding to the maximum rate of mass loss is identified from the peak of DTG curve. T_d represents the temperature at which degradation reactions proceed most rapidly. T_d is often used to compare the thermal stability of different epoxy formulations. A shift of T_d to higher temperatures indicates enhanced thermal resistance, whereas a shift to lower temperatures suggests accelerated degradation.

At high temperatures, the TGA curve approaches a plateau corresponding to the residual mass remaining after complete degradation of the organic matrix. This residue typically consists of char and inorganic filler content. In filled epoxy systems, the residual mass provides qualitative and quantitative information about filler loading and thermal shielding effects. A higher char yield is generally associated with improved flame resistance and thermal stability [12,13].

In filled epoxy composites, inorganic fillers typically enhance thermal stability by acting as heat barriers and promoting char formation. The residual mass at high temperatures can be used to estimate filler content and inorganic residue. TGA is therefore a critical tool for evaluating the long-term thermal reliability of epoxy materials used in microelectronic applications.

1.2.6 Adhesion Strength

The tensile lap-shear test is a widely used mechanical method for evaluating the adhesion performance of structural adhesives and polymeric bonding materials. This test measures the shear stress required to cause failure in a bonded joint by applying a tensile load parallel to the adhesive layer. Lap-shear strength is particularly relevant

for assessing the mechanical reliability of epoxy-based adhesives used in structural, electronic and microelectronic applications.

The lap-shear strength is influenced by several factors, including adhesive formulation, curing conditions, surface preparation of the substrates, adhesive thickness, and testing environment. For epoxy systems, crosslink density and interfacial bonding play a dominant role in determining shear resistance. A well-cured epoxy adhesive typically exhibits high cohesive strength, while insufficient curing or weak interfacial adhesion may lead to premature failure.

Failure modes observed during lap-shear testing provide additional insight into adhesion mechanisms. Cohesive failure within the adhesive layer indicates strong interfacial bonding, whereas adhesive failure at the interface suggests insufficient chemical or mechanical interaction with the substrate. Mixed-mode failure, involving both cohesive and adhesive characteristics, is commonly observed in filled epoxy systems and reflects a balance between bulk and interfacial properties.

In particle filled epoxy adhesives, the incorporation of inorganic fillers can affect lap-shear performance. At moderate filler loadings, improved stress transfer and crack deflection mechanisms may enhance shear strength. However, excessive filler content or poor dispersion can introduce stress concentration sites, leading to reduced adhesion strength. Therefore, lap-shear testing serves as a critical tool for optimizing filler type and loading level in epoxy based adhesive formulations.

1.3 Previous Studies on the Effects of Nitride and Oxide Particles

Literature survey on the isothermal curing kinetics revealed the effects of aluminum nitride [14,15], aluminum oxide [16], and silicon oxide [17]. In these studies, various dispersion methods such as direct mixing [15], bead milling [16] and sol-gel approach [17] were used. Improving filler dispersion and filler-matrix compatibility using these techniques were proven to be very important.

Ma *et al.* [14] studying the curing behaviour revealed that although the overall cure mechanism remained unchanged, the presence of AlN fillers reduced the reaction rate constants. This behaviour was attributed to restricted molecular mobility and increased viscosity at elevated filler contents, highlighting the trade-off between enhanced thermal transport and cure retardation in highly filled systems.

In contrast, Sanctuary *et al.* [16] focused on the effect of Al_2O_3 particles on the isothermal curing behaviour of an epoxy resin using temperature-modulated DSC and rheological measurements. Their study showed that Al_2O_3 particles accelerated the early stages of network formation, leading to faster macromolecular growth and earlier chemical vitrification. This acceleration was attributed to surface hydroxyl groups on the nanoparticles and enhanced local concentrations of reactive species near the filler surfaces. However, increasing nanoparticle content resulted in a reduction of the total reaction enthalpy, suggesting diffusion limitations at later stages of cure. These findings emphasize the strong influence of nanoparticle–matrix interactions on epoxy cure behaviour, particularly under isothermal conditions.

Yang *et al.* [17] examined the effects of SiO_2 on curing behaviour, network structure, and thermal characteristics. DSC analysis revealed that the epoxy/SiO_2 systems followed an autocatalytic curing mechanism, similar to conventional epoxy systems. However, the presence of well-dispersed silica particles led to reduced reaction rates, which were attributed to steric hindrance and partial consumption of epoxy groups during silica network formation. Complementary solid-state NMR and TEM analyses confirmed the formation of a highly crosslinked silica network within the epoxy matrix, demonstrating that fillers can significantly alter both the cure behaviour and the final network architecture of epoxy systems.

Hutchinson *et al.* [15] investigated epoxy composites filled with AlN, with particular emphasis on the relationship between cure behaviour and thermal conductivity for different curing chemistries (epoxy–amine and epoxy–thiol systems). The study highlights that the impact of fillers on cure behaviour is strongly dependent on the curing chemistry and interfacial characteristics

Literature survey revealed that aluminum nitride [14,15,18–23], aluminum oxide [21,23–31] silicon nitride [22,32,33], and silicon oxide [20,34] can be used at very high volume filler fractions (50-70 vol%) in overcoming the intrinsically low thermal conductivity of neat epoxy (≈0.17–0.22 W/m·K). It is demonstrated that the thermal conductivity of epoxy composites is fundamentally governed by filler type, volume fraction, morphology, and interfacial characteristics. An early work underscored the trade-off between improved conductivity and reduced processability when incorporating fillers [21].

Ma *et al.* [14] investigated epoxy/AlN composites with the primary objective of improving thermal conductivity while examining the influence of AlN fillers on cure behaviour using isothermal methods. Their results demonstrated that the incorporation of AlN significantly increased the thermal conductivity of the epoxy matrix, reaching values approximately five times higher than neat epoxy at high filler loadings.

It is shown that AlN is very effective in increasing thermal conductivity due to its superior intrinsic conductivity. It was reported that a thermal conductivity of ~4 W/m·K at ~62 vol% AlN and 7.15 W/m·K at 68.5 vol% AlN [21] was observed while a sharp percolation-driven increase at 65–70 vol% AlN was reported which yields conductivities five to eight times higher than equivalent silica-filled systems [19]. This behaviour was attributed to the efficiency of particles in establishing conductive networks within the matrix. At lower loadings, more modest improvements were demonstrated with nanoparticulate AlN raising conductivity from 0.168 W/m·K (neat epoxy) to ~0.199 W/m·K at 10 wt%, while validating the Agari–Uno model as the best predictive framework.

Many studies demonstrate that incorporating Al_2O_3 substantially increases the thermal conductivity of epoxy. At high loadings, micro-sized Al_2O_3 fillers raise conductivity to values between 0.6–1.3 W/m·K, depending on particle size, morphology, and dispersion quality. Extending this approach, the conductivities of 6.7 W/m·K is achieved with 79 vol% Al_2O_3 addition to epoxy [28]. Nano- Al_2O_3 can further improve thermal transport at low to moderate concentrations by reducing interfacial resistance although agglomeration risks limit its effectiveness at higher fractions. Predictive models show that AlN and Al_2O_3 filled systems up to 25 vol% highlights accompanying improvements in dielectric and thermo-mechanical stability [25].

The incorporation of $Si_3 N_4$ results in high thermal conductivity [22,34]. $Si_3 N_4$ nanowires could transform the thermal performance of epoxy matrices, achieving up to 9.2 W/m·K at 60 vol% with aligned nanowires by establishing efficient one-dimensional heat conduction networks [32].

It is reported that SiO_2 -filled epoxies achieved modest thermal conductivity (0.70 W/m·K at 65 wt%). The study demonstrated that nano-SiO_2 inclusions improved thermal uniformity but contributed little to conductivity gains, with discrepancies from theoretical predictions attributed to interphase effects around nanoparticles that hinder phonon transfer [34].

All studies highlight the need for dense packing and percolated filler networks to achieve significant thermal conductivity enhancements. It is consistently reported that spherical or large particles reduce resin-barrier effects, while poor interfaces depress conductivity. Modeling efforts appear across multiple studies, underscoring the importance of predictive frameworks, while practical issues such as viscosity, processability, and hydrolysis reappear as shared limitations. Achieving high thermal conductivity in particle-filled epoxies requires optimizing filler content, particle size and distribution, and interfacial compatibility.

Literature survey revealed that the thermal expansion coefficient (α) is lowered with the addition of aluminum nitride [19], aluminum oxide [25,35–39], silicon nitride [33,40], and silicon oxide [34,38–42] fillers. Thermal expansion coefficient is a key parameter in epoxy composites for electronic packaging, as it determines the magnitude of thermal stresses when bonded to other substrates. Neat epoxy typically exhibits a high α in the range of 50–90 $\times 10^{-6}$ /K**,** which is far greater than that of

semiconductor materials such as silicon (~4 × 10^{-6} /K), resulting in significant mismatch stresses during thermal cycling.

Dilatometry and TMA are commonly used to measure α and monitor materials' dimensional stability with changing temperature. It is demonstrated that incorporating up to 60 vol% AlN into epoxy reduces the composite α toward 4–5 × 10^{-6} /K, while simultaneously increasing λ above 4 W/m·K [43] and minimizing fatigue failures in semiconductor devices [19]. Besides, Al_2O_3 fillers progressively lower α with increasing filler fraction (0–25 vol%), alongside improvements in dimensional stability [25,36]. SiO_2 has been extensively investigated as a filler in epoxy composites to reduce α due to its low cost. It is showed that increasing SiO_2 loading consistently lowered α of epoxy systems while improving mechanical reliability [34]. The incorporation of Si_3N_4 into epoxy systems has been shown to significantly reduce α, achieving values in the range of 23–30 × 10^{-6} /K [40].

It is also demonstrated the micro-fillers are more effective in reducing α (down to 2.5 × 10^{-5} /K**)** than nano-fillers [38,39]. Nano-Al_2O_3 and nano-SiO_2 are reported to lower the composite α but the reductions were modest [37]. Besides, nanoscale additions are moderately reducing α in thin films; while high-volume fractions are effective in molding compounds [33,42].

Predictive modeling studies are also conducted to explain why measured composite α often deviate from simple mixture rules [35]. It is shown that filler–matrix interphase zones strongly influence α reductions.

Comparative analyses of epoxy composites reinforced with AlN, Al_2O_3, Si_3N_4, and SiO_2 demonstrate distinct differences in their ability to suppress thermal expansion. AlN exhibits the strongest α reducing effect owing to its intrinsically low α (~4–5 × 10^{-6} /K). Studies consistently report that AlN filled epoxies achieve substantial α reductions at moderate filler loadings (40–60 vol.%). Al_2O_3, although widely used due to low cost and good availability, is less effective; its higher intrinsic α (~7–8 × 10^{-6} /K) limits dimensional control, and α reductions are only moderate even at high loadings. Si_3N_4 provides low α (~3 × 10^{-6} /K) and excellent mechanical reinforcement. Its effectiveness, however, is somewhat below that of AlN because of less favorable dispersion and higher processing costs. SiO_2 , the most commonly employed filler, provides only modest α reduction due to its relatively higher intrinsic α and weaker interfacial stiffening compared to nitrides. High loadings (≥60 vol%) of silica are generally required to approach the α levels of silicon, but such additions compromise processability. In summary, the relative effectiveness of these fillers in suppressing the thermal expansion coefficient in epoxy matrices can be ranked as AlN > Si_3N_4 > Al_2O_3 > SiO_2. Among them, AlN demonstrates the highest efficiency owing to its combination of intrinsically low thermal expansion and high thermal conductivity, whereas SiO_2, despite being the most economically viable and widely adopted, provides the least reduction in α and thus represents the least effective option for dimensional stabilization.

Literature survey revealed that the addition of aluminum nitride [34,44], aluminum oxide [37,45,46], silicon nitride [33], and silicon oxide [34,41,45,47–50] affects thermal degradation temperature of neat epoxy.

Thermal degradation behaviours of filled epoxy systems are investigated by TGA which provides essential insight into their stability under operating temperatures.

With the addition of AlN, TGA curves of the composites remain more stable at higher temperature and the weight loss of the filled samples decreases with the addition of the AlN [44]. High-loading micro Al_2O_3 elevates the 5% weight-loss temperature ($T_{5\%}$) from 332°C for neat epoxy to 366°C indicating a substantial suppression of early mass loss under N_2 . For Si_3N_4 , thin-film epoxy composites exhibit degradation onsets clustered near ~350°C and T_5 % values that differ little from controls at low volume fractions, implying limited impact on the initial mass-loss threshold in those formulations [33]. SiO_2 additions yield a modest but consistent rise in TGA. For 1–5 wt% SiO_2 coatings, the temperature of 5% weight loss and the maximum decomposition temperature both increase by roughly 8–9°C relative to neat epoxy, which is attributed to inhibited chain mobility and improved char formation [50].

It is showed that epoxy nanocomposites containing AlN and SiO_2 nanoparticles displayed higher degradation onset temperatures than neat epoxy, exhibiting delayed weight loss due to interphase-induced restrictions on chain mobility [34]. Moderate filler loadings (3–7 wt.%) of SiO_2 results in the optimal thermal degradation resistance in epoxy/SiO_2 systems. It is also reported that high filler loadings (>30 wt.%) of SiO_2 could reduce cross-linking density, leading to localized decreases in decomposition temperatures [49].

The addition of Al_2O_3 and SiO_2 improved thermal stability, raising the onset of degradation by ~15–20°C compared to neat epoxy and significantly lower weight loss [33]. It is also reported that epoxy/SiO_2 composites exhibited significant increases in decomposition temperature, with a maximum enhancement of approximately 20.8°C at 5 wt.% loading [48].

Liang and Wong [31] examined epoxy composites containing micro- and nano-scale Al_2O_3 fillers. Although the study primarily focused on thermo-mechanical performance rather than direct thermal conductivity measurements, the authors reported that Al_2O_3 -filled systems exhibited superior thermal stability and higher storage modulus than corresponding SiO_2 filled systems. These results indirectly suggest improved heat resistance and thermal transport capability.

Across the studies, it is seen that inorganic fillers raise epoxy's thermal degradation temperature to differing extents. TGA results highlight that oxide and nitride fillers systematically increase thermal degradation temperature by 15–40°C and reduce overall weight loss during pyrolysis. Among them, Al_2O_3 and AlN are the most effective for bulk stabilization while SiO_2 is better in reducing mass loss and Si_3N_4 contributes moderate stability improvements in thin-film systems. In addition, the studies show that thermal degradation resistance is governed not only by filler chemistry but also by particle size, dispersion state, and the strength of filler–matrix interphases.

Literature survey revealed that loss factor ($tan\ \delta$) of epoxy can be modified with the incorporation of aluminum nitride [34], aluminum oxide [31,36,37,51–54], silicon nitride [22], and silicon oxide [31,34,50,55–57] fillers.

DMA is the most used technique to observe $tan\ \delta$ across the studies. It is demonstrated that the incorporation of fillers into epoxy resins significantly influences glass transition temperature. The extent and direction of the effect depend on filler type, size, and surface chemistry.

It is observed that Al_2O_3 additions (10–30 wt.%) improved T_g, with the highest values attained at 30 wt.%, where T_g increased in parallel with modulus, suggesting effective load transfer between filler and matrix [58].

It is reported that Al_2O_3 particles, even at relatively low loadings (1 wt.%), markedly enhanced the storage modulus due to restricted polymer chain mobility, while T_g was modestly shifted upward, reflecting increased crosslink density in the cured network [31,53].

It is showed that incorporating 5-7 wt.% SiO_2 increased T_g from 48.9°C in neat epoxy to 51.3-58.2°C**,** attributing this gain to effective interfacial adhesion and chain immobilization [50,55]. Another study revealed that 2-8 wt.% SiO_2 nanoparticles shifted T_g upward by 4-6°C**,** but noticed that loadings above 10 wt.% led to nanoparticle agglomeration, reducing reinforcement efficiency [57].

1.4 Aim of This Thesis

Epoxy resins are one of the most significant subclasses of thermosetting polymers having the key functional group of epoxide rings. In the industry, the most common type of epoxy resin is based on the crosslinking reaction of DGEBA with an amine type curing agent. That type of epoxy resin has a wide range of applications including paints, coatings, adhesives, and of course as the matrix material of fiber reinforced structural composites. Moreover, in the electronics industry, these epoxy resins are used for certain parts of many microelectronic devices.

In the microelectronic applications of epoxy resins, mainly there are two points that must be investigated; (i) curing behaviour and (ii) thermal properties. Isothermal curing behaviour is especially significant to determine optimum parameters of time & temperature required for efficient curing procedure of the components during their production. Thermal properties of epoxy systems such as thermal conductivity, thermal expansion coefficient, glass transition temperature, thermal degradation temperature are also very critical for the performance of those microelectronic parts which are under severe heating & cooling cycles during their operations.

In certain ordinary applications, use of neat epoxy resins might be sufficient for these requirements. For the advanced microelectronic applications, investigators improve performance of epoxy resins by adding certain particles. Researchers try to use so many different type, form, size of organic particles being especially nitrides and oxides.

In this respect, in order to improve curing behaviour and thermal properties of epoxy resin, four different particles preferred in this study were aluminum nitride (AlN), aluminum oxide (Al_2O_3), silicon nitride (Si_3N_4) and silicon oxide (SiO_2). Previous studies cited in the literature are summarized above in Section 1.3. Literature survey summarized in Section 1.3 revealed that only one type of particle is used for only isothermal curing behaviour and/or for one or two thermal properties.

Therefore, in order to contribute related literature much efficiently and in a comparative approach especially in terms of particle content, the main purpose of this study was to use all these four different particles with three different contents; for both isothermal curing behaviour and for all thermal properties (thermal

conductivity, thermal expansion coefficient, glass transition temperature, thermal degradation temperature) of epoxy resin.

Additionally, since proper adhesion of these epoxy based parts in microelectronic devices are crucial, effects of all these four particles on the adhesion strength were also analyzed, which was often neglected in the literature.

CHAPTER 2

EXPERIMENTAL WORK

In this study, experimental works conducted could be simply grouped into five main stages: (i) size-range determination of the fillers used, (ii) production of the particle filled epoxy samples, (iii) calorimetry analysis of the samples for isothermal curing behaviour, (iv) various analyses of the specimens for thermal properties, and lastly (v) adhesion strength measurements necessary for the epoxy based parts used in microelectronic devices. Experimental techniques used in each step were summarized below.

2.1 Epoxy Resin System and Oxide / Nitride Particles Used

Epoxy resin and curing agent system especially preferred in microelectronic devices chosen were Diglycidyl Ether of Bisphenol-A (DGEBA) type epoxy with Trimethyl-1, 6-Hexadiamine type curing agent (EPO-TEK 301, Epoxy Technology Inc., USA) (Figure 2.1). Four different fillers used were aluminum nitride (AlN, purity 99.95%), aluminum oxide (Al_2O_3, purity 99.5%), silicon nitride (Si_3N_4, purity 99.5%) and silicon oxide (SiO_2, purity 97.3) particles (Nanografi Nanotechnology Inc., Turkey) (Figure 2.1).

In this study, neat epoxy system (designated as EP) was filled with 10, 20 and 40 wt% of each particle. Thus, specimen designation style used for the filled epoxy was EP/AlN x% , EP/ Al_2O_3 x% , EP/ Si_3N_4 x% , and EP/ SiO_2 x% , respectively; where x% indicates the amount of the particles used in wt%.

In the present study, the filler contents were intentionally expressed in terms of weight percent (wt%). This preference was mainly associated with the practical aspects of sample fabrication, since the preparation of epoxy specimens is fundamentally carried out through mass based measurements during weighing and mixing of the epoxy resin and filler particles. Therefore, defining the filler loading in wt% provides a direct and convenient representation of the experimental formulation used during specimen preparation.

Nevertheless, in particle filled polymer composites the microstructural interactions between the matrix and the filler particles are more closely related to their volumetric distribution within the polymer matrix. For this reason, the conversion between wt% and vol% can be preferred. The conversion can be performed by considering the densities of the epoxy matrix and the corresponding filler particles. Since ceramic fillers such as AlN, Al_2O_3 , $Si_3 N_4$ and SiO_2 generally possess significantly higher densities than the epoxy resin, a given wt% loading corresponds to a relatively lower volume fraction in the composite.

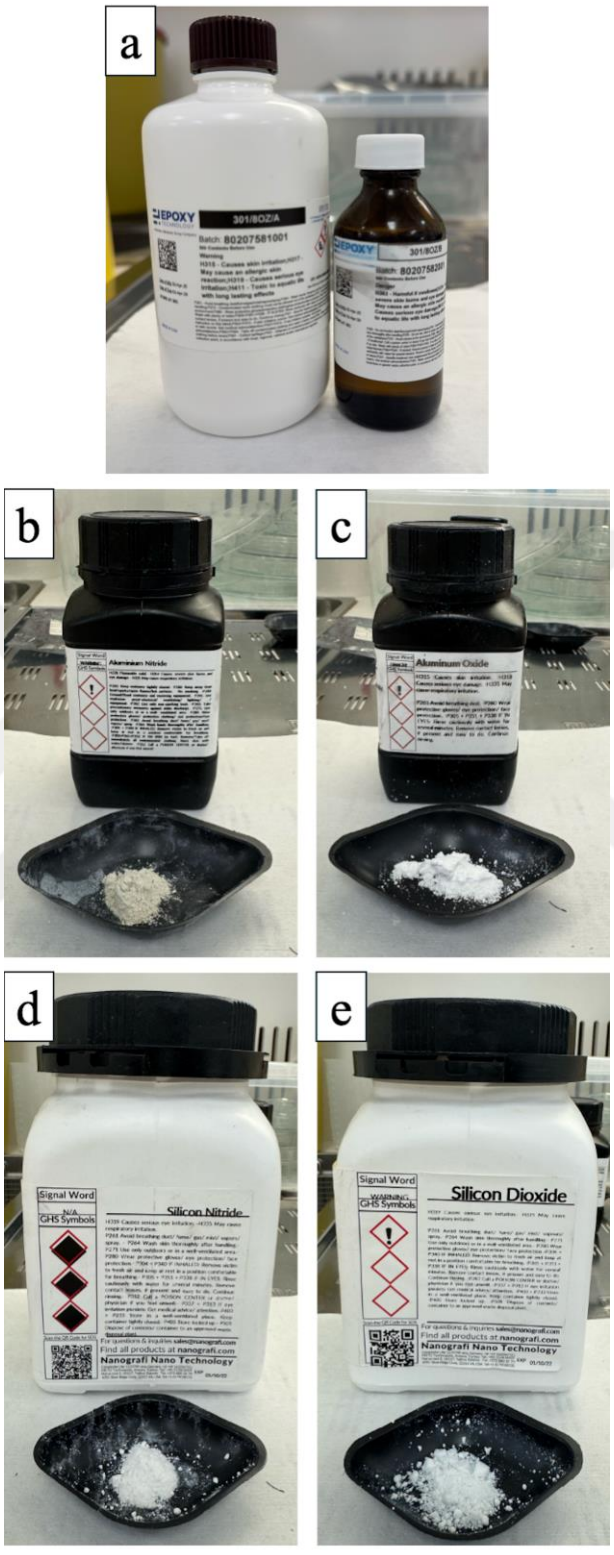

Figure 2.1. Materials used in this study; (a) epoxy resin and curing agent, (b) AlN, (c) Al_2O_3, (d) Si_3N_4 and (e) SiO_2 particles.

2.2 Dynamic Light Scattering (DLS) Analysis

In order to determine size distribution of the oxide and nitride particles, DLS (Malvern, Zetasizer Nano ZS, UK) (Figure 2.2) measurements were carried out in triplicate, at room temperature, by using 633 nm red laser. Samples were prepared by sonicating in isopropanol for 3 min prior to the measurements. During size distribution calculations, the values of refractive index used for AlN, Al_2O_3, Si_3N_4 and SiO_2 were 1.76, 2.15, 2.04 and 1.46 respectively.



Figure 2.2. DLS equipment used in this study.

2.3 Scanning Electron Microscopy (SEM) Analysis

Apart from DLS analysis, scanning electron microscopy (SEM, FEI Quanta 3D 600 Dual Beam, USA) operating at an accelerating voltage of 20 kV was utilized as an additional technique to reveal morphology and size range of the filler particles adhered on double sided carbon tapes which were sputtered with gold to minimize electrostatic charging (Figure 2.3).

It should be noted that, SEM analysis was also used to examine the fracture surfaces of certain broken specimens in order to observe the degree of filler dispersion in the epoxy matrix. Since filled epoxy specimen are also not electrically conductive, they were again gold coated.

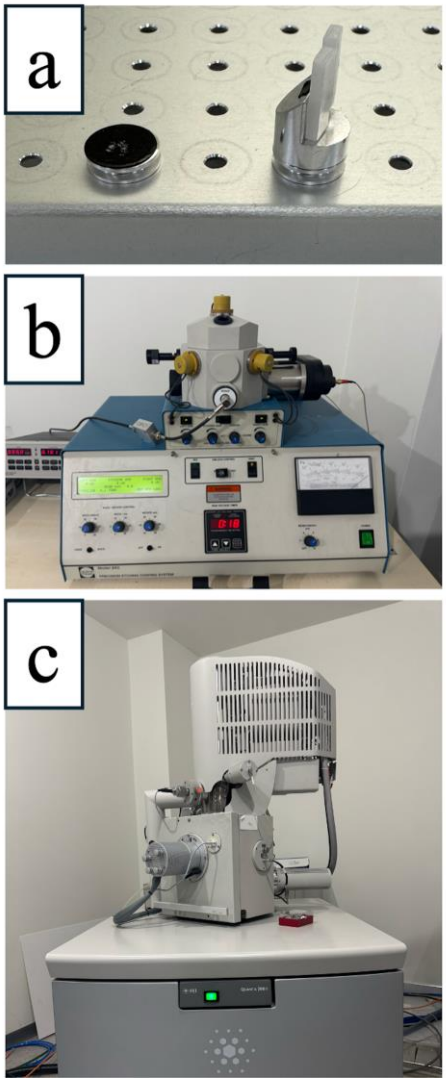

Figure 2.3. Sampling (a), gold sputtering (b) and main SEM equipment (c) used in this study.

2.4 Production of the Particle Filled Epoxy Samples

In this study as schematically illustrated in Figure 2.4 , epoxy based liquid samples and solid specimens required were produced by using two main stages.

(i) Mixing and Degassing:

Since viscosity of the resin systems starts to increase as soon as the curing agent added, leading to significant problems for homogeneous dispersion of the fillers; particles were first added to curing agent. In order to prevent agglomeration, this mixture was stirred properly with the help of an ultrasonic bath (Elmasonic, P180H, Germany) for around 20 min with the power of 250 W. Then, epoxy resin (in 4/1 ratio) was added to curing agent/particle mixture with further stirring this time using a magnetic stirrer (IKA, RCT Basic, Germany) with 100 rpm for 10 min. In order to get rid of bubbles formed during mixing, degassing operation was applied with further stirring by a speed mixer (FlackTek, DAC 1200-300 VAC, USA) at 2000 rpm for 5-10 min; of course in its proper vacuum chamber (Figure 2.5).

(ii) Liquid Sample or Solid Specimen Production:

After mixing and degassing main stage, two different paths were followed depending on the required liquid sample or solid specimen geometry for different analyses. In the first path, used for isothermal curing behaviour, it was very straight forward, i.e. filling of DSC pans just after degassing step (Figure 2.6).

On the other hand, in the second path used for the production of solid specimens required to determine various thermal properties; two further steps were necessary, i.e. specimen molding and then curing. For this purpose, first flexible molds having the required cavity for each testing method were produced using polydimethylsiloxane elastomer. After filling those molds with liquid resin systems prepared before, it was necessary to apply curing procedure at 80°C for 6 h in a furnace (Memmert, VO29, Germany) to obtain solid rigid specimens (Figure 2.7).

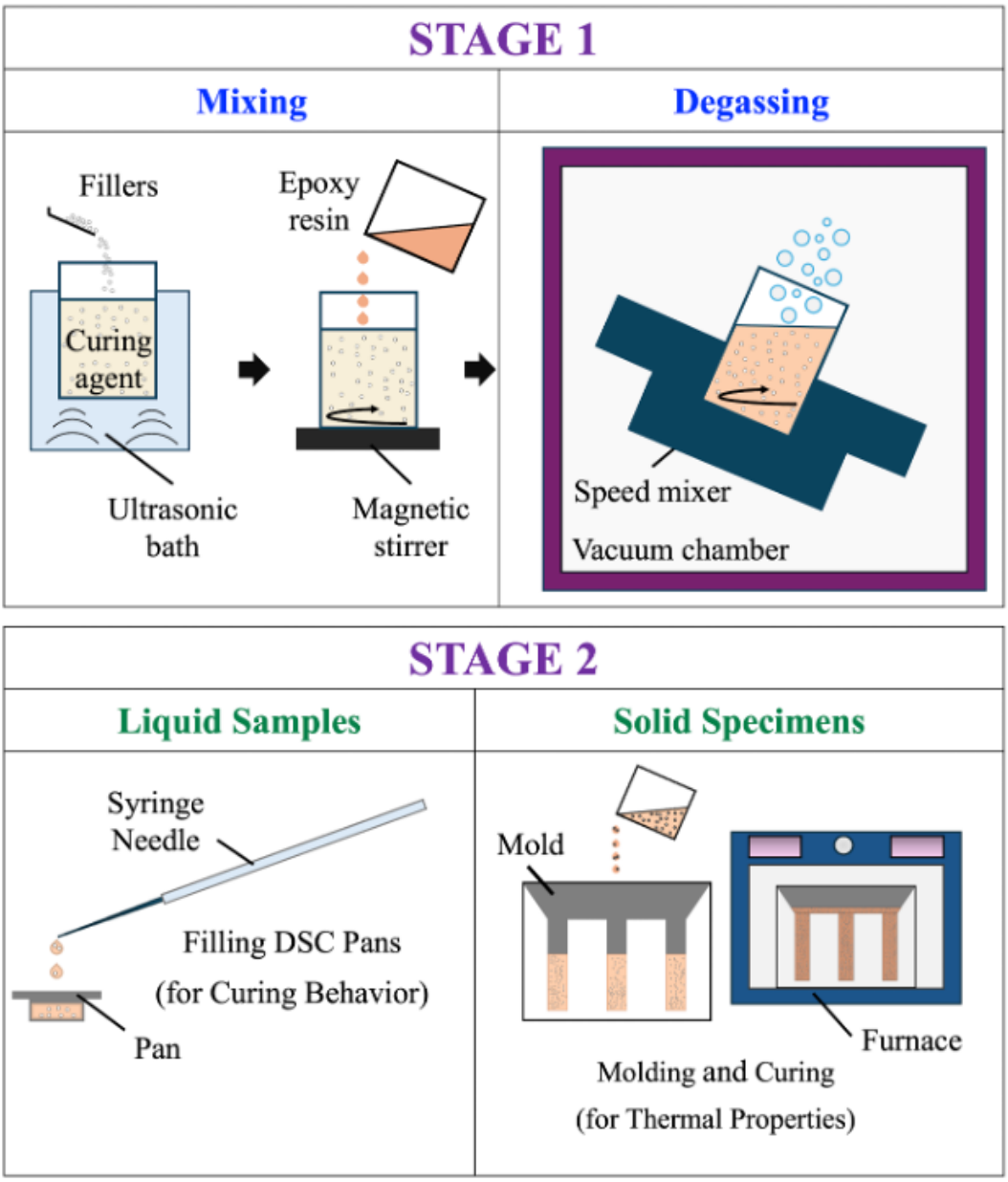

Figure 2.4. Two main stages used for the production of liquid samples and solid specimens.

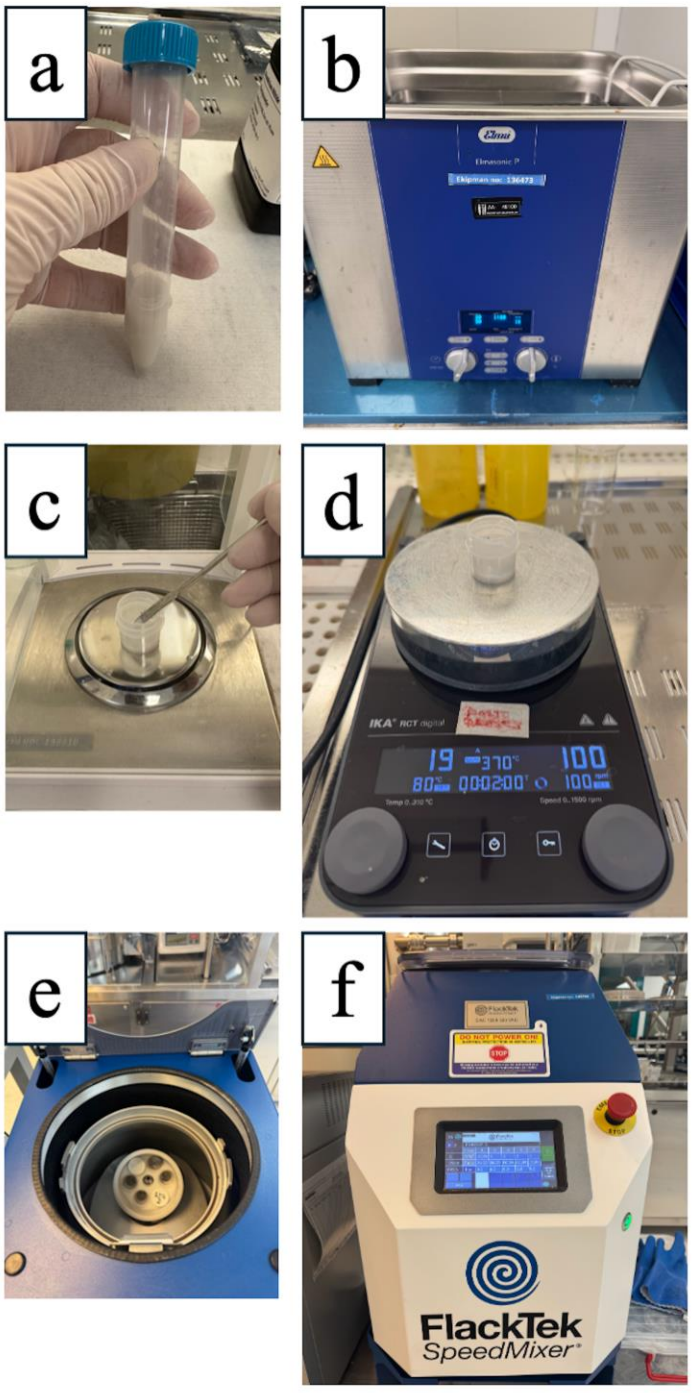

Figure 2.5. Equipment used in stage 1; (a) mixing of fillers into the curing agent, (b) ultrasonic bath, (c) adding epoxy resin into the mixture, (d) magnetic stirrer, (e,f) sample holder and speed mixer equipment used in this study.

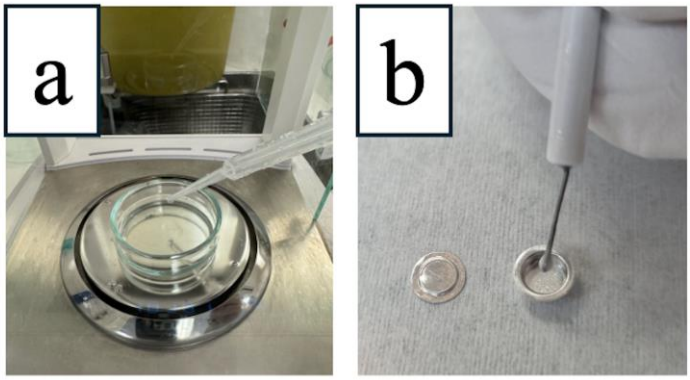

Figure 2.6. Equipment used in stage 2 for liquid samples; (a) mixing of epoxy resin and curing agent and (b) filling DSC pans by using syringe needle.

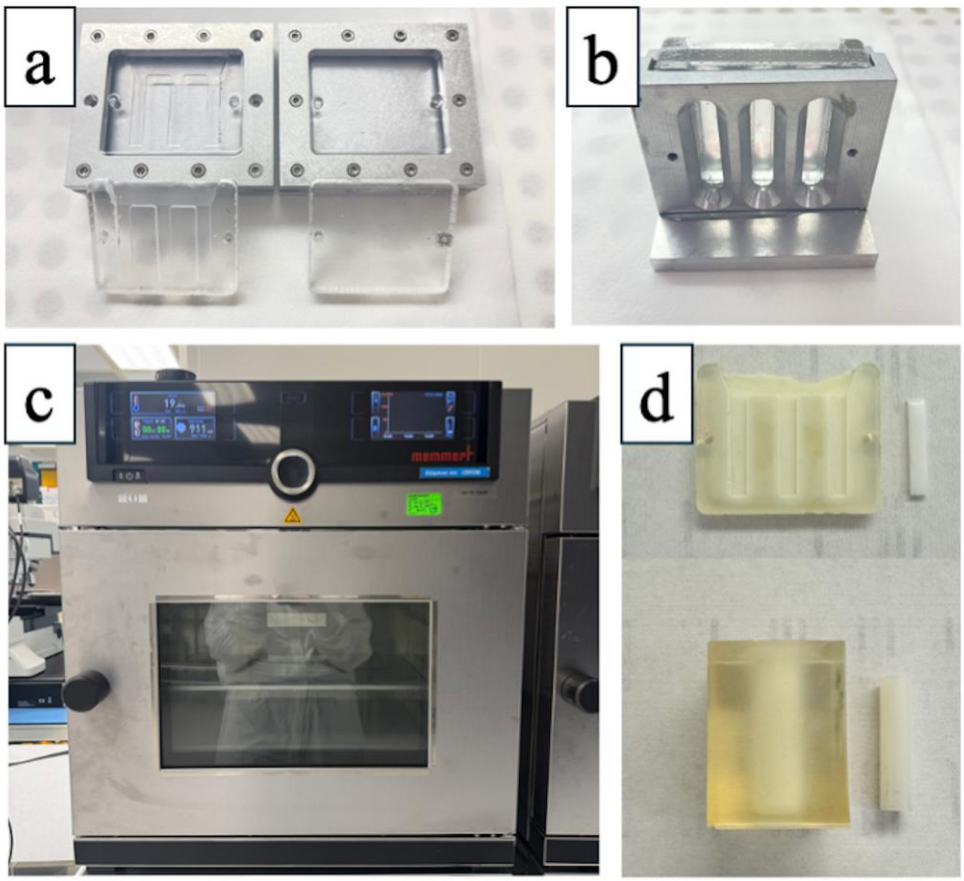

Figure 2.7. Equipment used in stage 2 for solid specimens; (a) master molds to produce molds, (b) mold in vertical holder, (c) curing furnace and (d) solid specimens after curing in molds.

2.5 Differential Scanning Calorimetry (DSC) Analysis

DSC analyses (TA Instruments, DSC Q2000, USA) (Figure 2.8) with samples of 2–10 mg in sealed aluminum pans were conducted by recording heat flow as a function of time. All procedures were performed under nitrogen flow of 50 ml/min. Analyses were conducted to investigate effects of filler particles on the isothermal curing behaviour of epoxy system. For this purpose, all samples were isothermally kept at 80°C for around one hour.

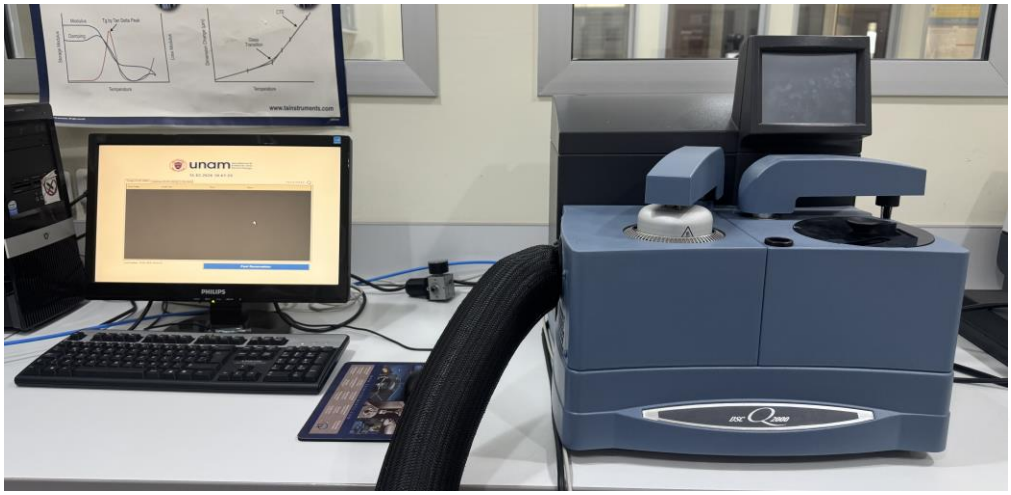

Figure 2.8. DSC equipment used in this study.

2.6 Thermal Conductivity Analysis

In order to reveal effects of filler particles on the thermal properties of epoxy system, the first analysis conducted was Thermal Conductivity measurements. Neat and each filled epoxy samples were molded and cured into disc shaped specimens with the diameter of 50 mm and thickness of 2 mm according to ASTM E1530 standard [59]. Prior to the measurements, specimens were conditioned at room temperature and 50% relative humidity for 24 hours. After applying a known heat pulse, temperature rise at the surface was recorded and analyzed using the software of instrument (TA

Instruments, DTC-300, USA) (Figure 2.9) to determine their thermal conductivity values. All measurements were carried out at ambient temperature.



Figure 2.9. Thermal conductivity measurement equipment used in this study.

2.7 Dilatometry Analysis

Dilatomery (Netzsch, DIL 402 Expedis Supreme, Germany) (Figure 2.10) was the second thermal analysis used for all specimen types in order to determine their Thermal Expansion Coefficient values. Cylindrical specimens having the length of 30 mm and diameter of 10 mm were molded and cured in accordance with ASTM E228 standard [60]. Specimens were first cooled down to -180°C and then heated to 70°C with cooling & heating rate of 10°C/min.

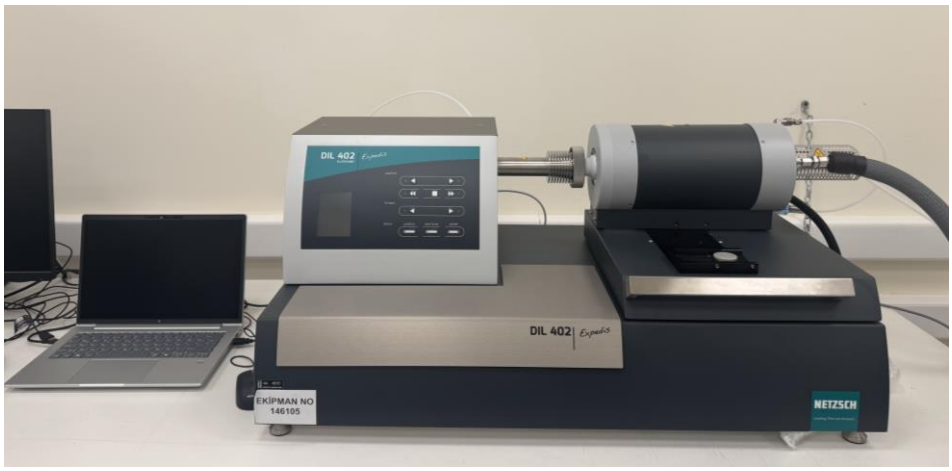

Figure 2.10. Dilatometry equipment used in this study.

2.8 Dynamic Mechanical Analysis (DMA)

Thirdly, in order to observe effects of particles on the Glass Transition Temperature of the epoxy system, DMA (TA Instruments, DMA Q800, USA) (Figure 2.11) analysis of the bar shaped (30×5×2 mm) molded specimens under single cantilever mode, from Room Temperature to 100°C with a heating rate of 5°C/min were conducted to determine especially *tan δ* curves. Moreover, changes in the mechanical stiffness of the specimens were evaluated by using the values of Storage Modulus (E') at 25°C and 50°C.



Figure 2.11. DMA equipment used in this study.

2.9 Thermogravimetric Analysis (TGA)

As the fourth analysis, to reveal effects of particles on the Thermal Degradation Temperature of epoxy system, TGA (TA Instruments, TGA Q500, USA) (Figure 2.12) analyses were conducted. For this purpose, 5–10 mg specimen pieces in platinum pans were heated up to 800°C at a heating rate of 10°C/min under nitrogen flow. Percent weight losses in each specimen were evaluated to determine values of their thermal degradation temperature.

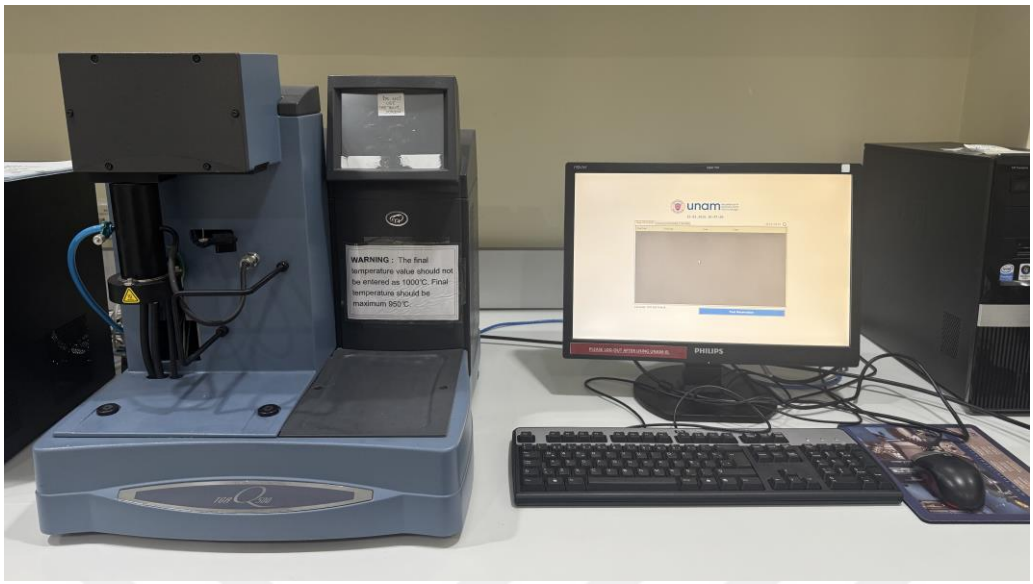

Figure 2.12. TGA equipment used in this study.

2.10 Lap Shear Adhesion Tests

In many electronic devices, since epoxy systems were especially used for “adhesive or coating purposes”, effects of particle fillers on the epoxy system were investigated by conducting Lap Shear Adhesion tests in accordance with ASTM D1002 standard for all specimen combinations [61].

Aluminum alloy plates (100×25×1mm) used as adherent, were first carefully cleaned with acetone and isopropanol in an ultrasonic cleaner (Elma, Elmasonic Select 80, Germany). Then, neat and filled liquid epoxy resin samples prepared were uniformly applied and pressed in between two aluminum plate adherents carefully; by using a proper alignment fixture, so that the same bonding area (12.5×25 mm) could be maintained for each combination.

After curing the specimen system at 80°C for 6 h in an oven, tensile loads (with a rate of 0.5 mm/min) were uniformly applied via the precise gripping of a Universal Test System (Instron 5969, USA) (Figure 2.13). Load versus displacement curves obtained during each test were evaluated to determine Lap Shear Strength (MPa) of

each specimen system by dividing the maximum in load (N) to the bonding area (mm2). Tests were repeated three times for each specimen combination. Failure modes (adhesive, cohesive, or mixed) after each test were also examined.

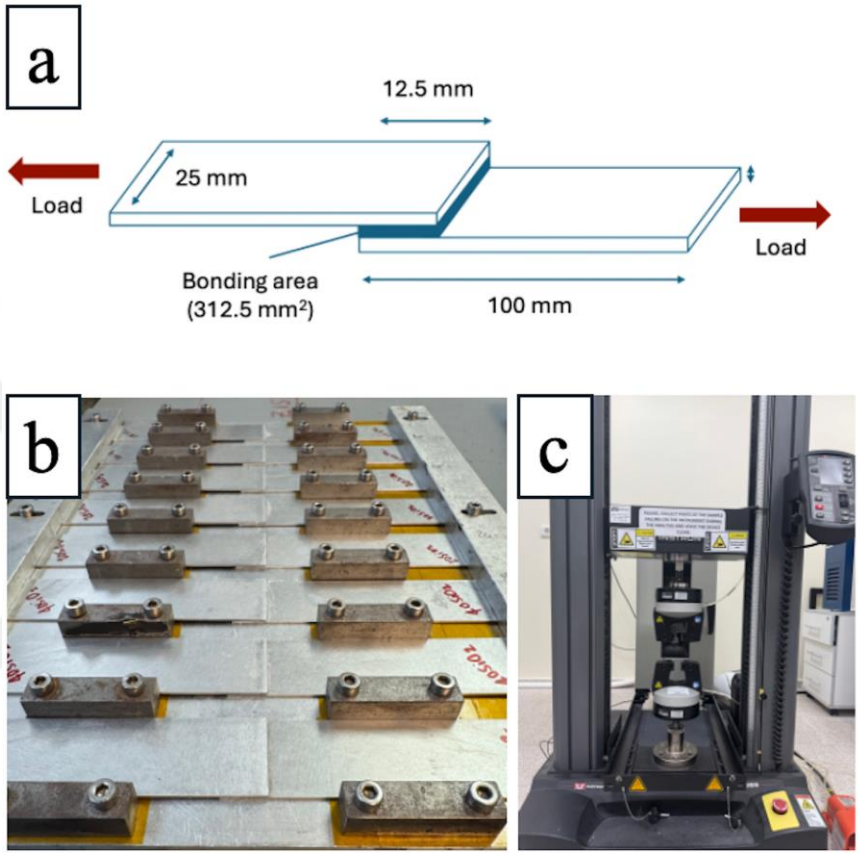

Figure 2.13. (a) Schematic showing the dimensions of lap shear adhesion test specimens, (b) Test specimens attached to the fixture (c) Universal Testing System used in this study.

CHAPTER 3

RESULTS AND DISCUSSION

After giving the results of size range and dispersion of oxide and nitride particles in the matrix; effects of each particle on the isothermal curing behaviour and thermal properties of epoxy resin system used in microelectronic devices were discussed one by one; including their adhesion strength.

3.1 Size Range and Dispersion of the Oxide and Nitride Particles in Epoxy Matrix

As shown in Figure 3.1, SEM analysis conducted to reveal size range and morphology of the particles indicated that their diameter range was 1-5 μm, which could be classified as "microparticles". It was also observed that, AlN particles had rather "polyhedral" morphology, while the other three had more "round" morphology.

Results of DLS analysis in the form of normal (Gaussian) type size distribution histograms given in Figure 3.2 revealed that the average particle size of AlN, Al_2O_3, Si_3N_4, and SiO_2 were 2341 nm, 1892 nm, 1211 nm, and 661 nm, respectively; which were consistent with the size range observed under SEM analysis.

In order to observe the degree of filler dispersion in the epoxy matrix, SEM analyses were also conducted on the fractured surfaces of each specimen combination having 10, 20 and 40 wt% particles. Since rather high filler contents were required for the

improvement of thermal properties, it was generally observed that particles were all dispersed in the matrix with certain degree of “agglomeration”. Figure 3.3 shows examples of 20 wt% particle dispersion in the epoxy matrix.

Bekeshev et al. [62] revealed that chemically modifying the surface of the fillers increases the chemical compatibility with the epoxy composition, thus provides better dispersion and mechanical characteristics. Similar observations were also discussed in other studies [47,63–67].

On the other hand, because of the “outgassing” problem that must be prevented in many microelectronic devices, no surface treatment was applied to the particles in this study. Examples of the microelectronic components in which “outgassing” is a key reliability concern are MEMS, sensors, optoelectronics, power modules etc. Therefore, no surface treatment agents or similar compounds were utilized so as to eliminate any risk of “outgassing” problem in this study.

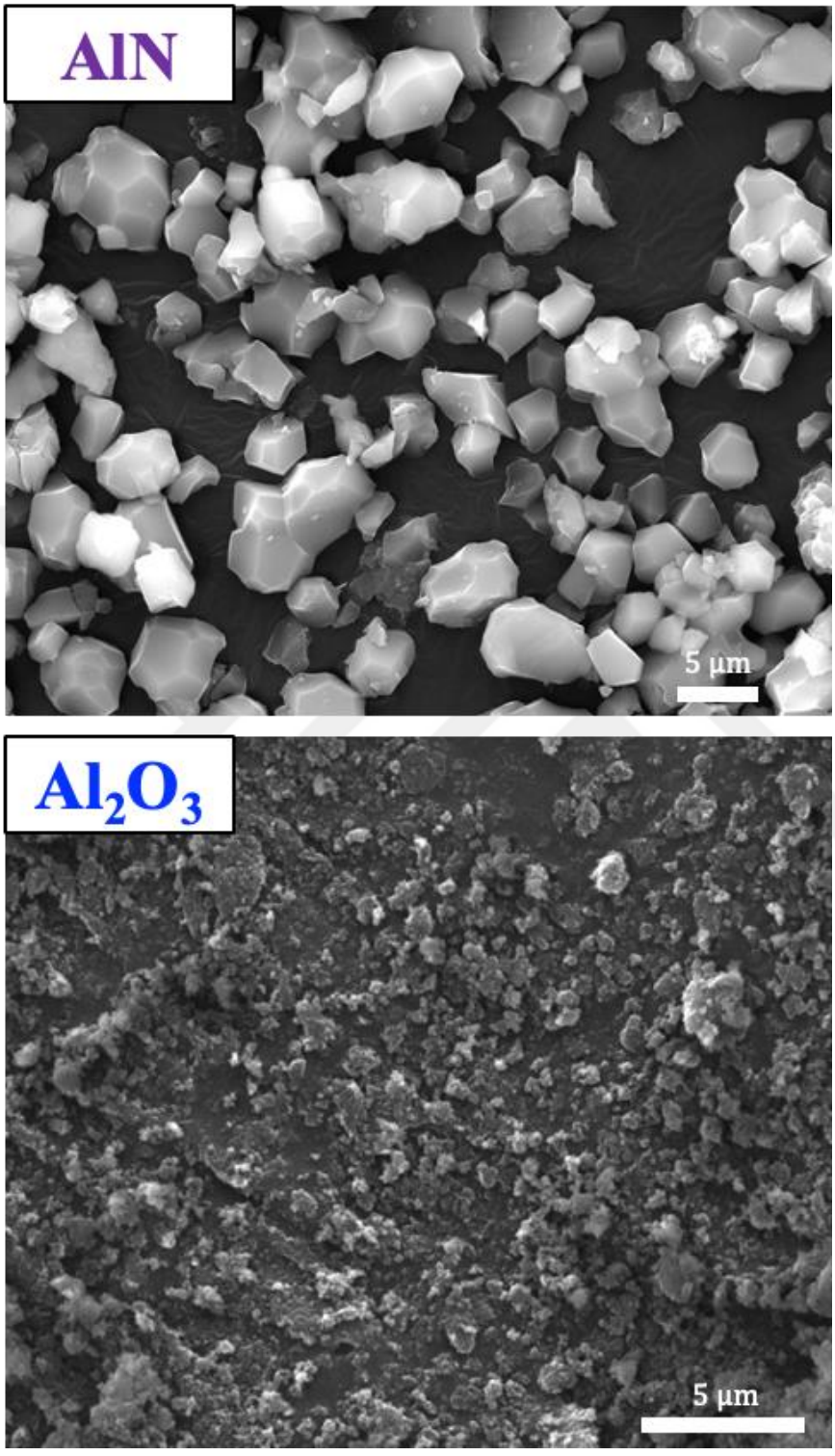

Figure 3.1. SEM images showing size range and morphology of the particles.

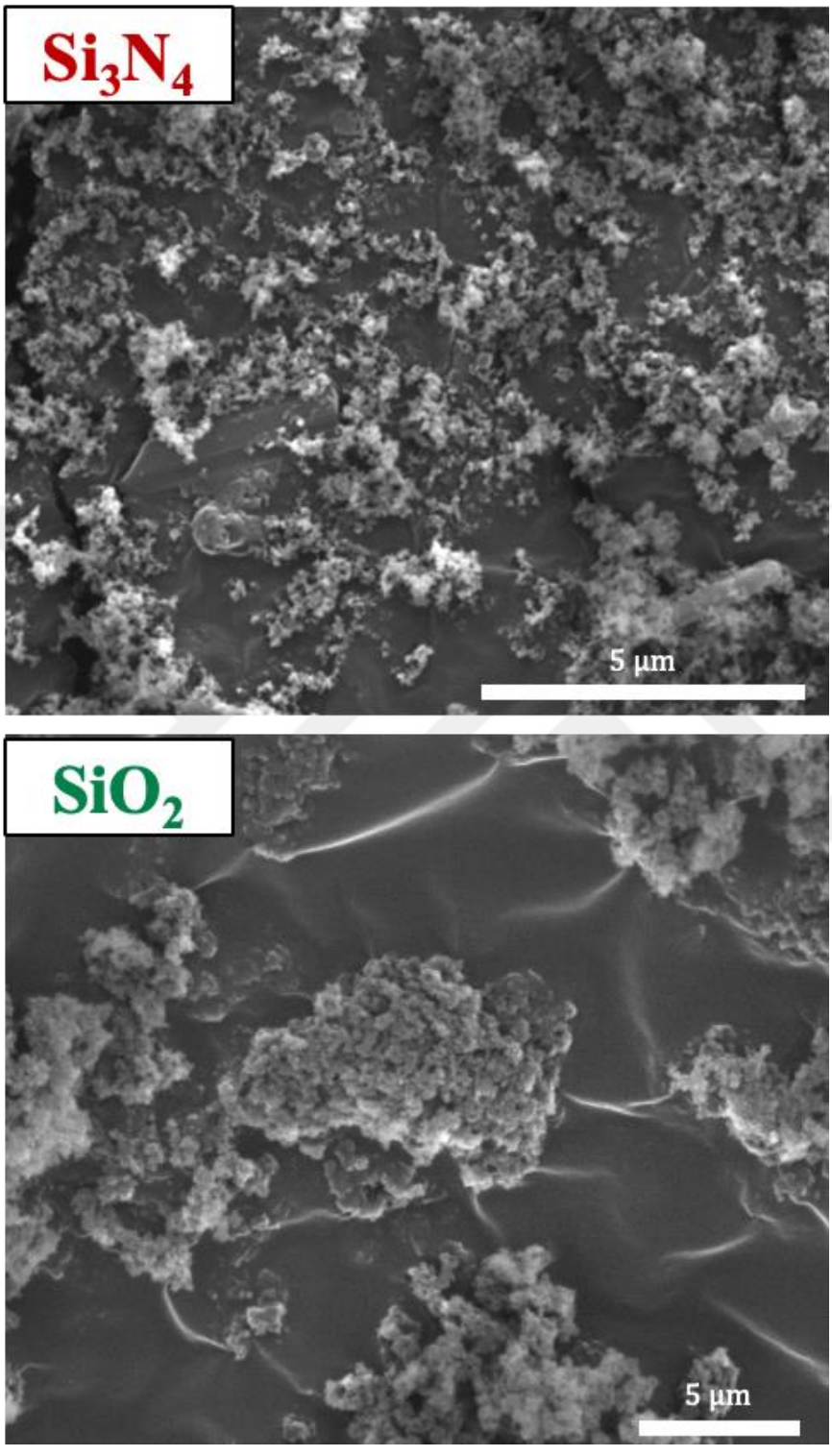

Figure 3.1. Continued.

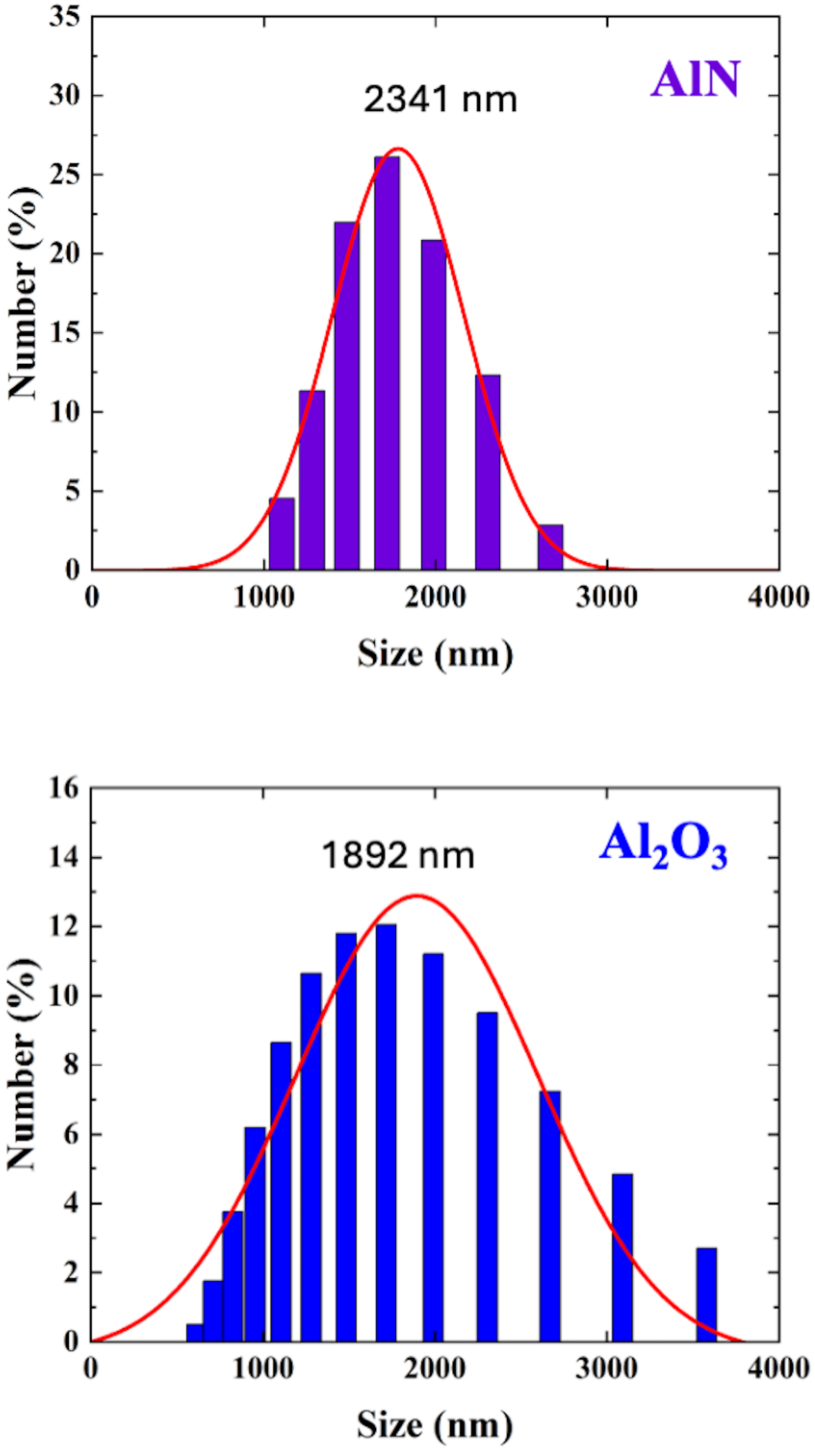

Figure 3.2. Size distribution of the particles determined by DLS analyses.

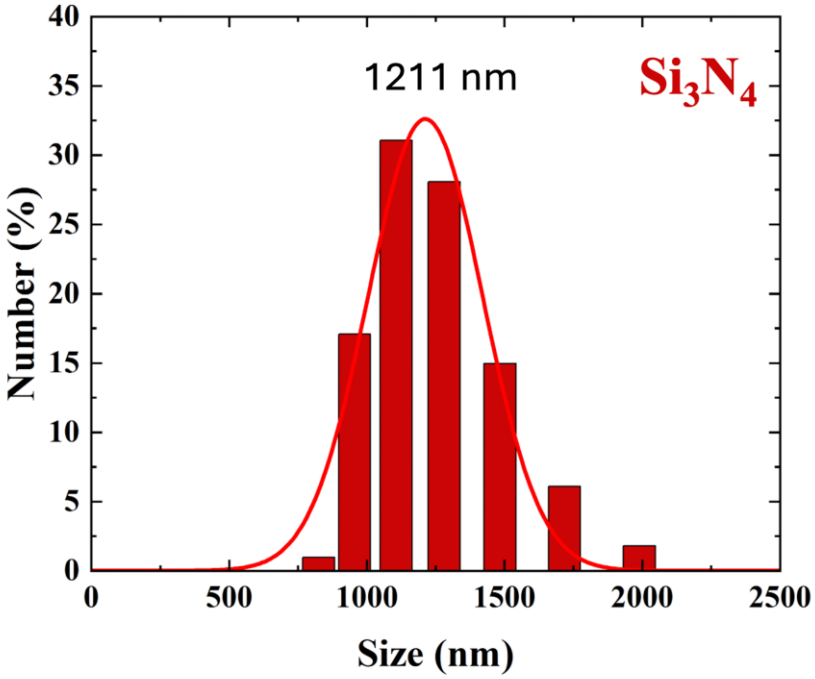

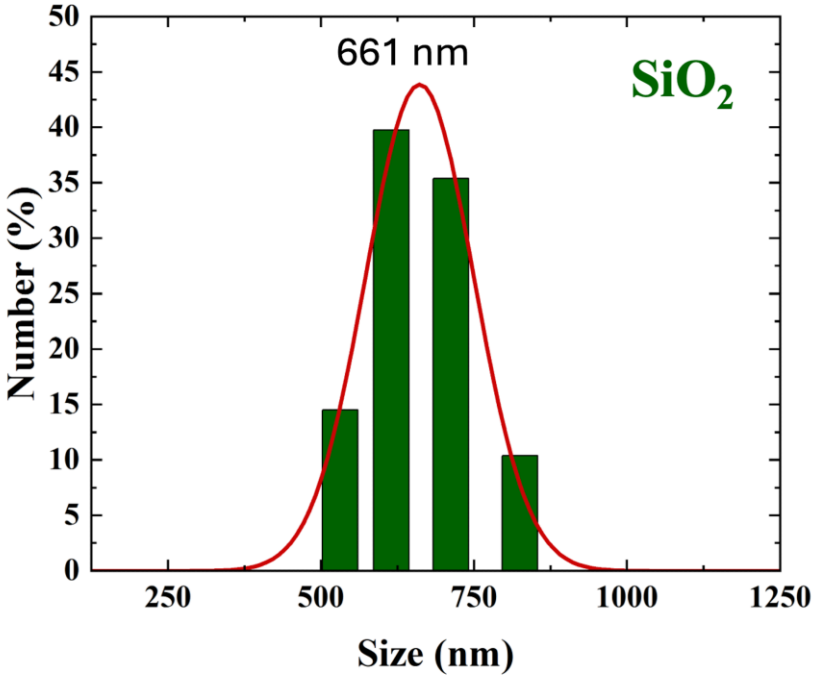

Figure 3.2. Continued.

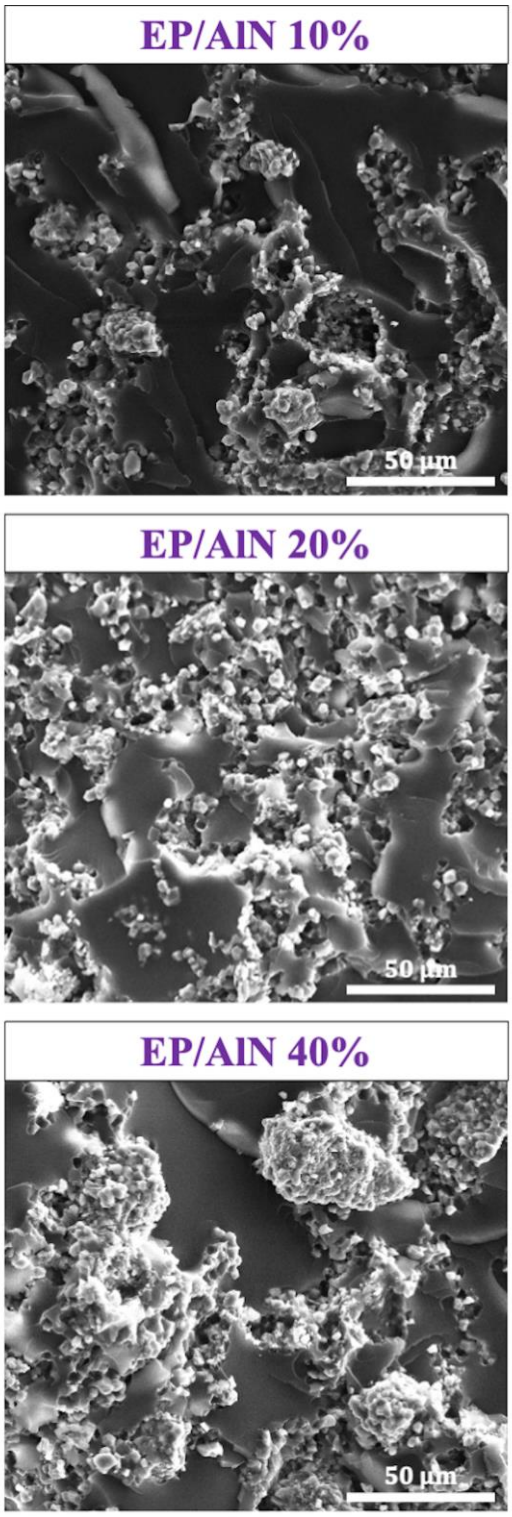

Figure 3.3. SEM images showing dispersion of particles in the epoxy matrix.

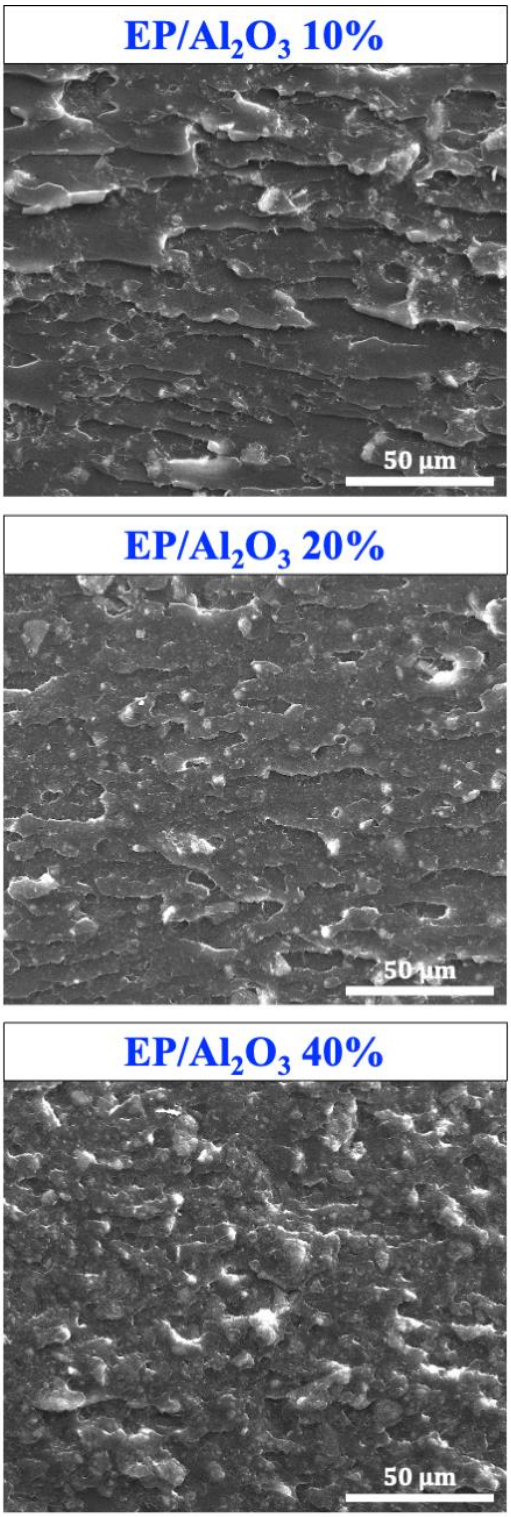

Figure 3.3. Continued.

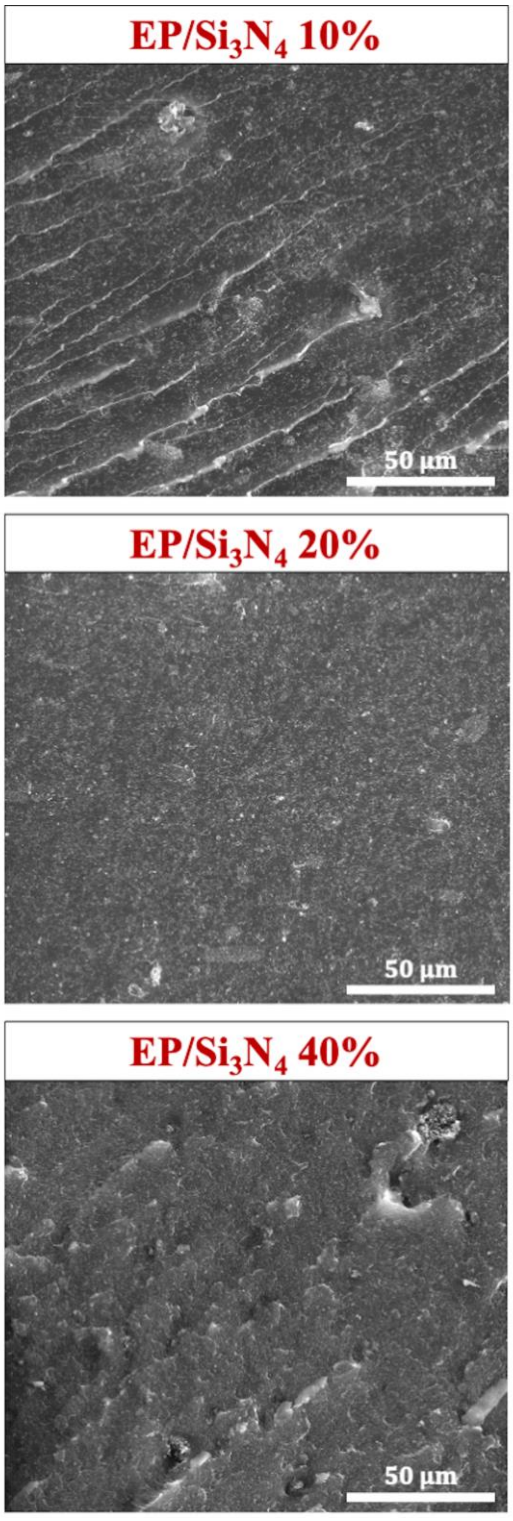

Figure 3.3. Continued.

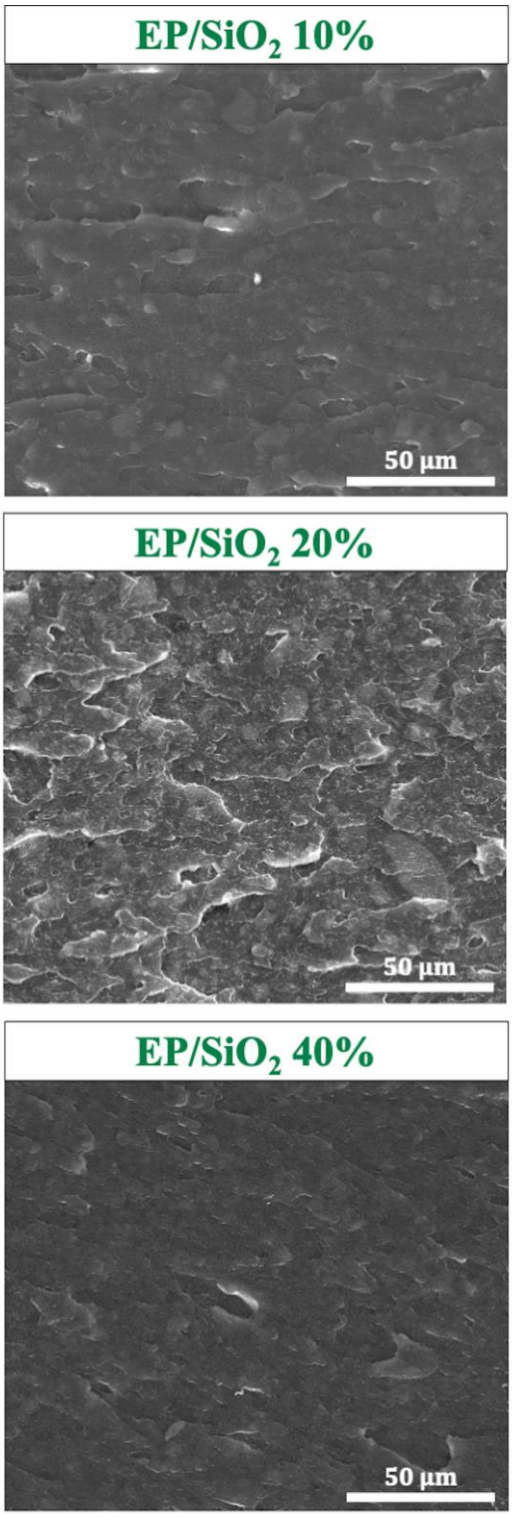

Figure 3.3. Continued.

3.2 Effects of Particles on the Isothermal Curing Behaviour

In the industrial applications including microelectronic devices, epoxy resin systems are generally cured isothermally at a certain temperature advised by the resin suppliers or according to the user experience; which was 80°C for the resin system used in this study. Therefore, in order to reveal effects of the oxide and nitride particles on the isothermal curing behaviour of the epoxy system, isothermal DSC analyses were conducted for all combinations of liquid samples at 80°C.

Heat Flow versus Time curves recorded for all filled samples were compared with the neat epoxy (EP) sample (Figure 3.4). It was observed that exothermic peaks of curing reaction decreased by increasing the amount of oxide and nitride particles used.

In practice, rather than the isothermal “Heat Flow” versus “Time” curves, it is more significant to obtain curing “Conversion” versus “Time” curves, so that effects of particles on the Isothermal Curing Behaviour could be revealed. For this purpose, data in Figure 3.4 were transformed into curing Conversion versus Time curves as given in Figure 3.5. Moreover, Conversion versus Time curves based on particle type and content are also presented in Figure 3.6.

Conversion percent for each point in Time was determined by the cumulative area between the curve of the thermogram and the x-axis, with respect to the overall heat of reaction. Moreover, all curves in Figure 3.5 were evaluated in terms of Time required for 50%, 75% and 100% curing Conversion in Table 3.1.

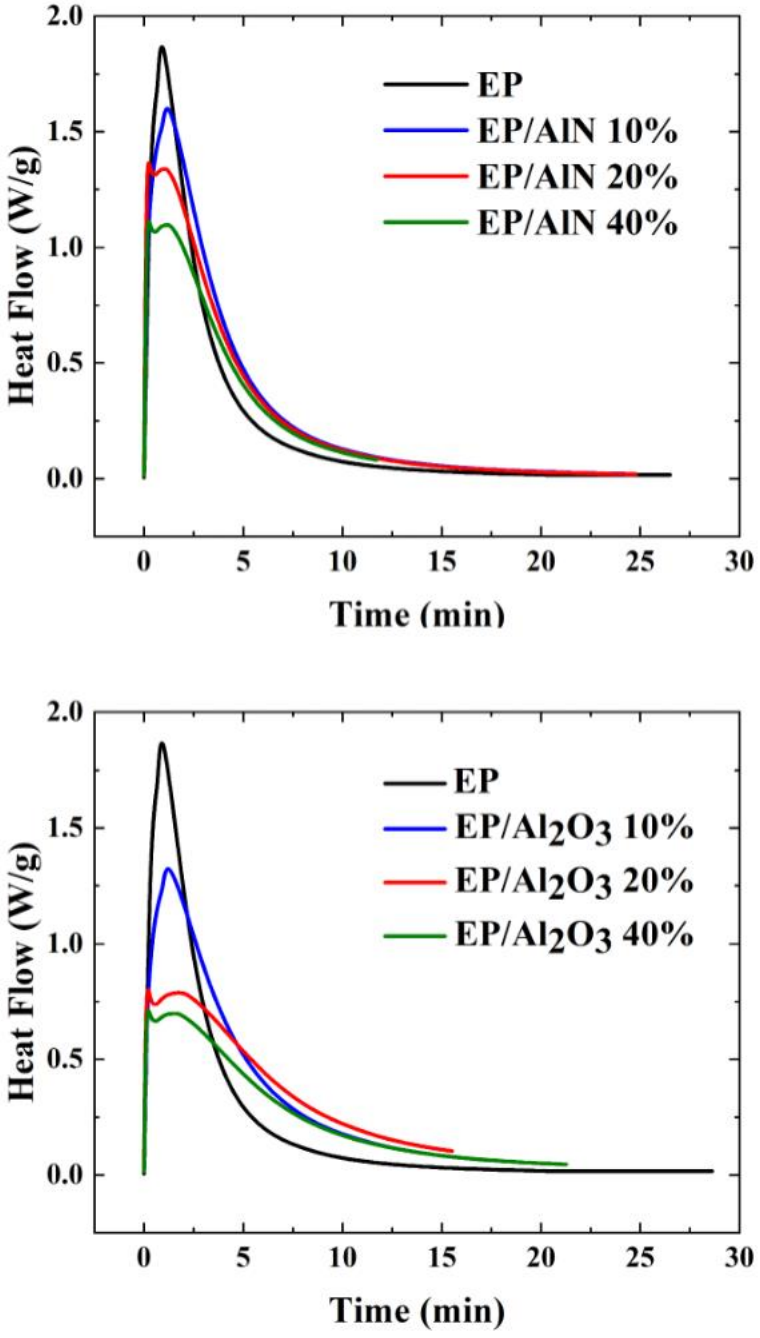

Figure 3.4. Effects of particles on the isothermal Heat Flow versus Time curves of epoxy.

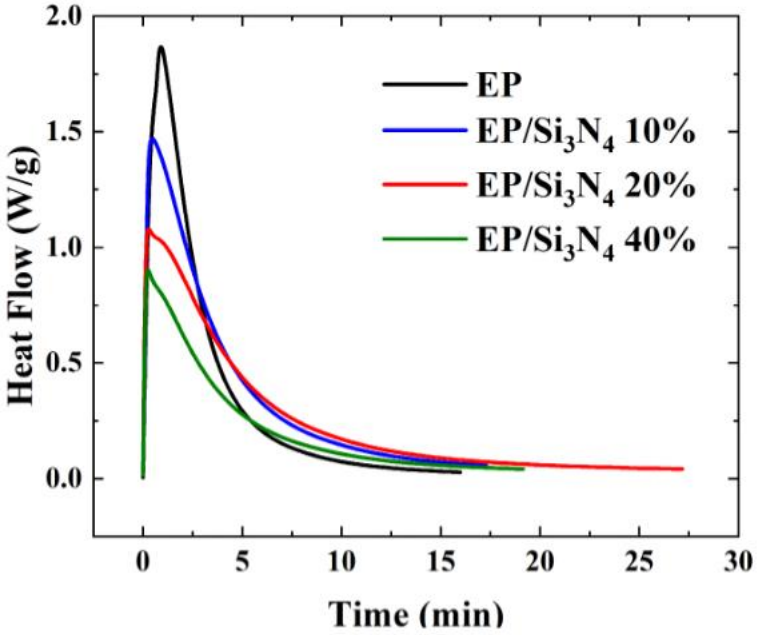

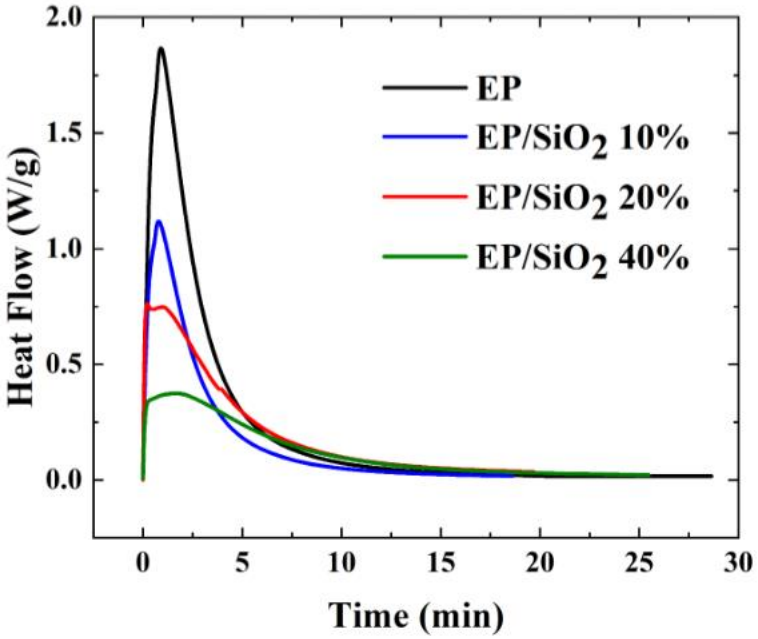

Figure 3.4. Continued.

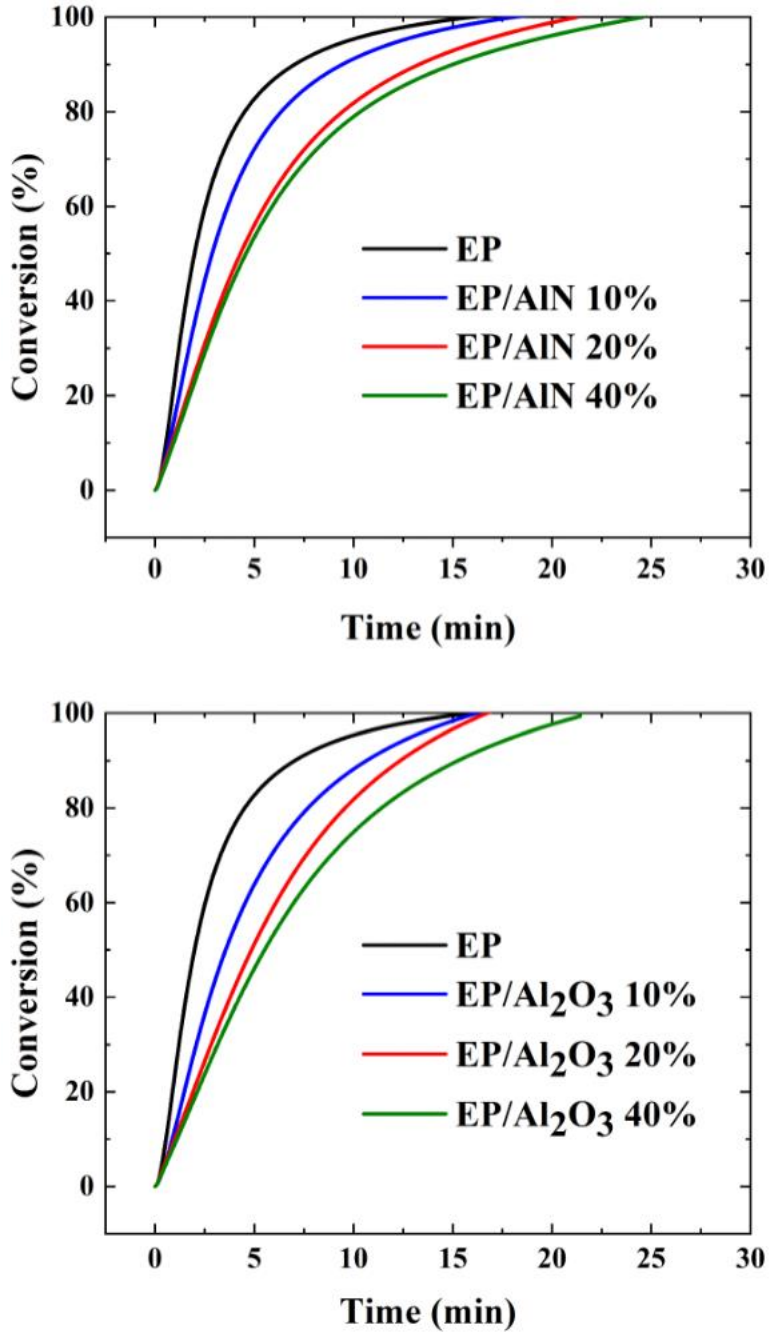

Figure 3.5. Effects of particles on the curing Conversion versus Time curves of epoxy.

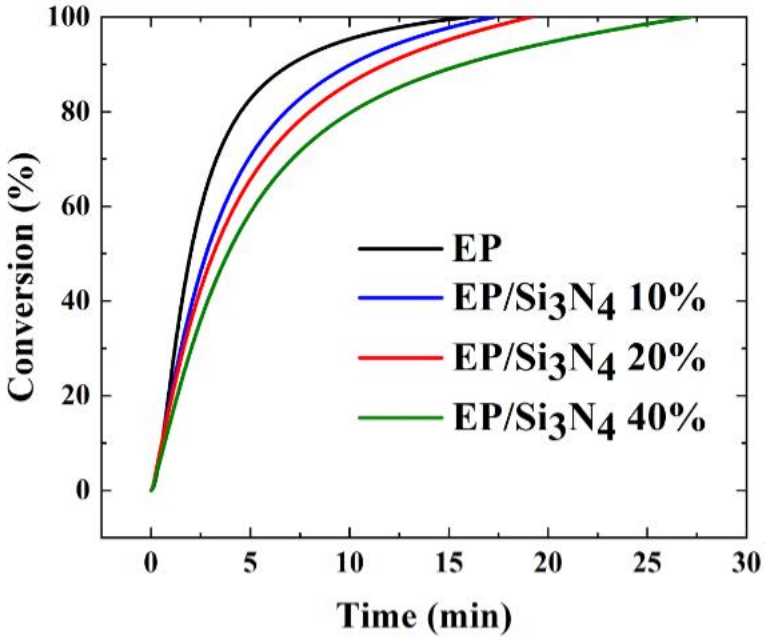

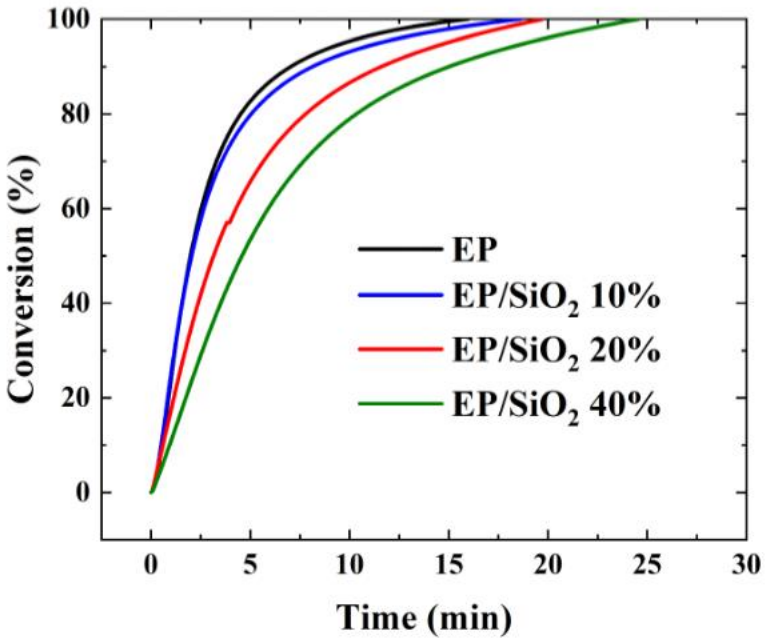

Figure 3.5. Continued.

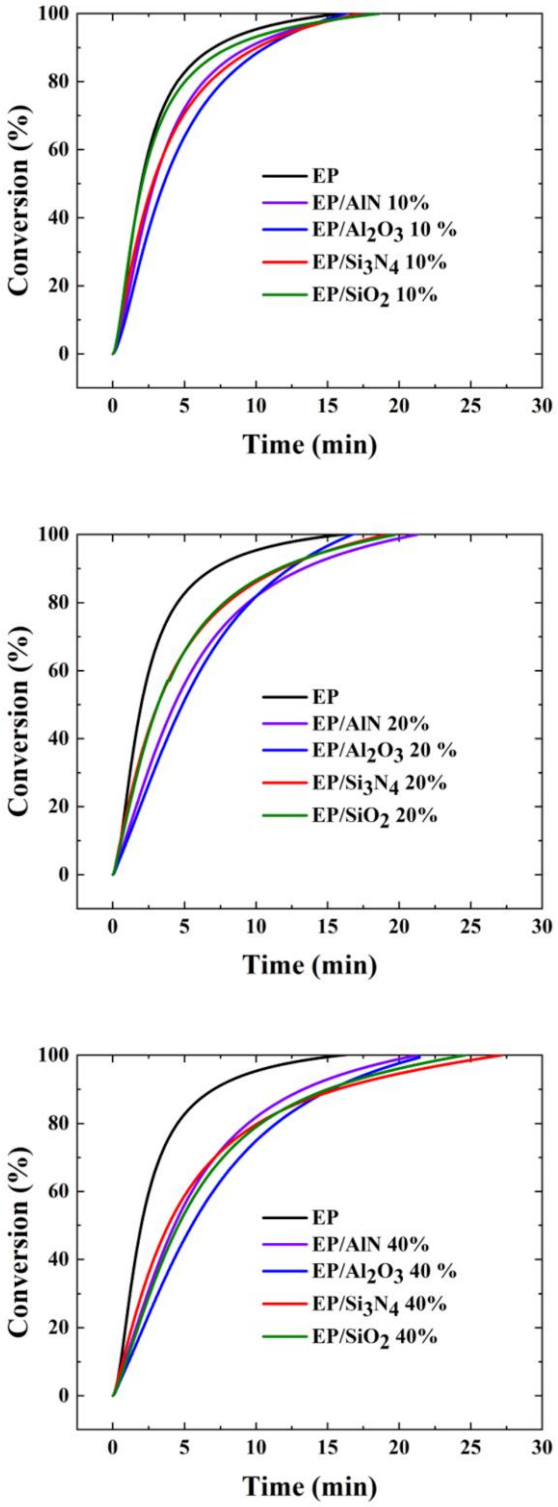

Figure 3.6. Effects of particle type and content on the curing Conversion versus Time curves of epoxy.

Table 3.1. Effects of Particles on the values of $t_{50\%}$, $t_{75\%}$ and $t_{100\%}$ (Time required for 50%, 75% and 100% curing Conversion)

	$t_{50\%}$ (min)	$t_{75\%}$ (min)	$t_{100\%}$ (min)
EP	2.1	3.9	16.1
EP/AlN 10%	2.9	5.4	18.1
EP/AlN 20%	4.4	8.4	21.3
EP/AlN 40%	4.6	9.1	24.6
EP/Al_2O_3 10%	3.6	6.7	16.2
EP/Al_2O_3 20%	4.9	8.6	16.7
EP/Al_2O_3 40%	5.6	10.2	21.4
EP/Si_3N_4 10%	2.9	5.7	17.3
EP/Si_3N_4 20%	3.2	6.9	19.1
EP/Si_3N_4 40%	3.9	8.4	27.2
EP/SiO_2 10%	2.2	4.3	18.6
EP/SiO_2 20%	3.2	6.6	19.8
EP/SiO_2 40%	4.6	8.9	24.6

Figure 3.5, Figure 3.6 and Table 3.1 revealed that incorporation of nitride and oxide particles into the epoxy resin all increased the time required for the isothermal curing conversion significantly. Delays in the conversion percent of isothermal curing was more pronounced at higher particle loading. For example, when particles were added as 40 wt%; time required for 50% curing conversion of neat epoxy increased from 2 min to up to 5 min; for the 75% curing conversion, time increased from 4 min up to 10 min; similarly for the 100% curing conversion, time increased from 16 min up to 27 min.

These retardations in time for the conversion percent of isothermal curing might be especially due to the physical constraint action of the particles leading to decreases in the segmental mobility of the epoxide and amine oligomers required for the

efficient cross-linking reactions during curing. Therefore, increasing the amount of the particles in the epoxy resin system increases the particle-induced steric hindrance leading to more delays during isothermal curing procedures.

It was observed that AlN , Al_2O_3 , $Si_3 N_4$ and SiO_2 particles all lead to reduction in the curing rate relative to neat epoxy, reflecting increased viscosity, reduced free volume, and diffusion-controlled limitations imposed by the particulate phases. At higher filler loadings, these effects become more pronounced for all systems, with extended reaction tails reflecting delayed network formation and vitrification.

However, the degree of this retardation also depends on filler chemistry and interfacial characteristics. Among the investigated fillers, AlN and $Si_3 N_4$ exhibit lower degree of suppression in the initial curing rate, particularly at moderate filler loadings, suggesting comparatively weaker restriction of epoxy–hardener mobility during early stages of curing. This behavior may be attributed to their lower surface polarity and more thermally conductive nature, which can promote more homogeneous heat distribution and reduce localized vitrification effects.

In contrast, Al_2O_3 and especially SiO_2 induce a more significant reduction in peak reaction rate and broader curing profiles, indicating dominant physical hindrance and stronger interfacial confinement. Because higher polarity on the surfaces of Al_2O_3 and SiO_2 likely enhance filler–matrix interactions, leading to constrained interphase regions that limit reactive group accessibility and accelerate the transition to diffusion-controlled kinetics. Similar observations discussed by Yang *et al.* [17] showed that SiO_2 incorporation reduced the cure rate due to steric hindrance from the inorganic network.

3.3 Effects of Particles on the Thermal Conductivity

When epoxy resins are used for the certain parts of microelectronic devices, the most significant property influencing its thermal performance would be the level of Thermal Conductivity (λ). Because heat development during operation of these devices should be released to the environment via heat diffusion which requires certain level of λ . Unfortunately, all polymers including epoxy have extremely low level of thermal conductivity, for instance for the neat epoxy resin used in this study it was determined as 0.15 W/m·K which was mainly due to the cross-linked network structure of thermosetting polymers leading to significant phonon scattering and limited heat transport pathways.

Since ceramic materials including the nitride and oxide particles used in this study have intrinsic thermal conductivity values much higher than 10 W/m·K, one of the best ways to improve thermal performance of epoxy resins would be incorporation of these particles.

Results of the thermal conductivity analyses shown in Figure 8 and Table 3 revealed that, although there were slight differences between each particle used, increasing the amount of all particles increased the thermal conductivity values. For example, when particles were added as 10 wt%; increases in the λ values were up to 80%; when 20 wt% particles were added increases were more than 2 times; while increases in the λ values were more than 3 times when 40 wt% particles were added.

Although more than three-fold increase of λ values (i.e. from 0.15 to 0.56 W/m·K) seem to be insignificant compared to the extremely high conductivities of metallic

materials, it would contribute to the thermal performance of microelectronic parts made from particle-filled epoxy, significantly. Because heat development during operation of these devices would be released more than three-fold easier compared to the parts made from neat epoxy. In the literature of particle-filled epoxy systems [14,28,30,34,68–70], very similar λ increases up to around 0.40 - 0.50 W/m·K were also reported. These improvements in the λ values with increasing particle content can be at-tributed to the progressive formation of thermally conductive pathways within the epoxy matrix. As the nitride and oxide particle content increases, particle–particle interactions become more significant, facilitating the formation of certain conductive pathways that reduce phonon scattering at the polymer–filler interfaces and improve overall heat transport.

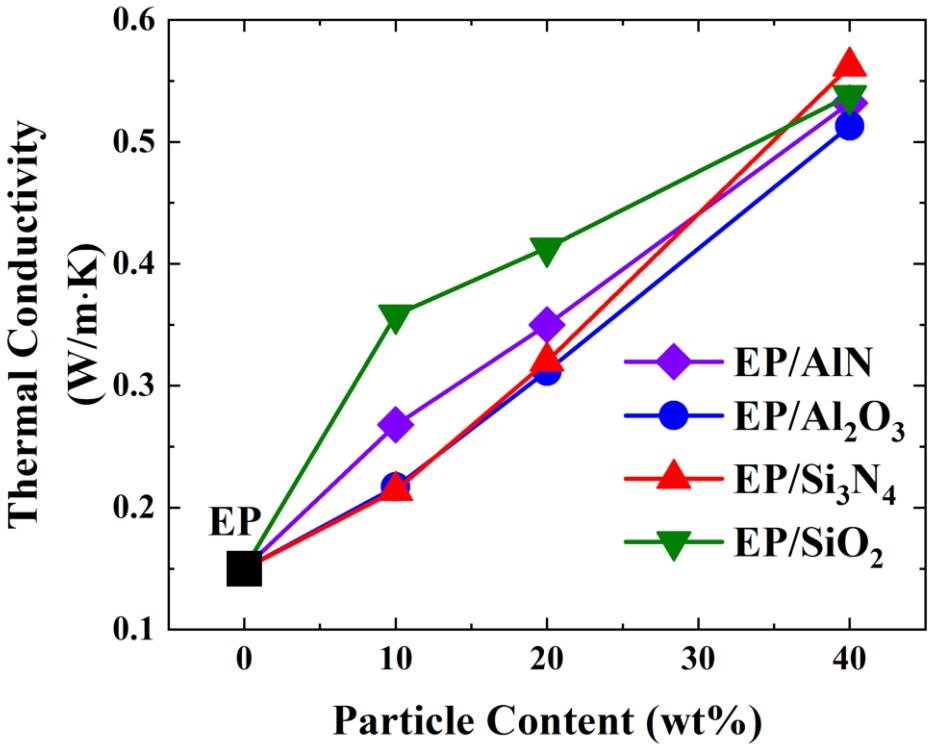

Figure 3.7. Effects of Particles on the Thermal Conductivity of Epoxy.

3.4 Effects of Particles on the Thermal Expansion Coefficient

Another significant problem in terms of thermal performance of microelectronic devices arises when there are different parts made with different materials. Because heat development during operation of these devices would lead to "*thermal strain mismatch*" due to the different values of Thermal Expansion Coefficient (α) of each material used in the device. If the degree of "*thermal strain mismatch*" reaches above the acceptable design limits, then the microelectronic device loses its dimensional stability leading to malfunctioning.

Thus, when epoxy resins are used for the certain parts of microelectronic devices, another significant property influencing its thermal performance would be the level of thermal expansion coefficient (α). Unfortunately, all polymers including epoxy have extremely high level of α, for instance for the neat epoxy resin used in this study it was determined as 49×10^{-6}/K. Since nitride and oxide ceramic particles used in this study have thermal expansion coefficient (α) values much lower than 10×10^{-6}/K, one of the best ways to improve thermal performance of epoxy resins by decreasing its α value would be again incorporation of these particles.

Results of the thermal expansion coefficient analyses shown in Figure 3.8 and Table 3.2 indicated that, although there were slight differences between each particle used, increasing the amount of all particles decreased the thermal expansion coefficient values. For example, when particles were added as 10 wt%; decreases in the α values were down to 42×10^{-6}/K (i.e. decrease of -15%); when 20 wt% particles were added decreases were down to 38×10^{-6}/K (i.e. decrease of -33%); while decreases in the α values were down to 28×10^{-6}/K (i.e. decrease of -43%) when 40 wt% particles were

added. In the literature, significant decrease in the α values (23–30×10^{-6} /K) were reported [40] after the incorporation of Si_3N_4 particles.

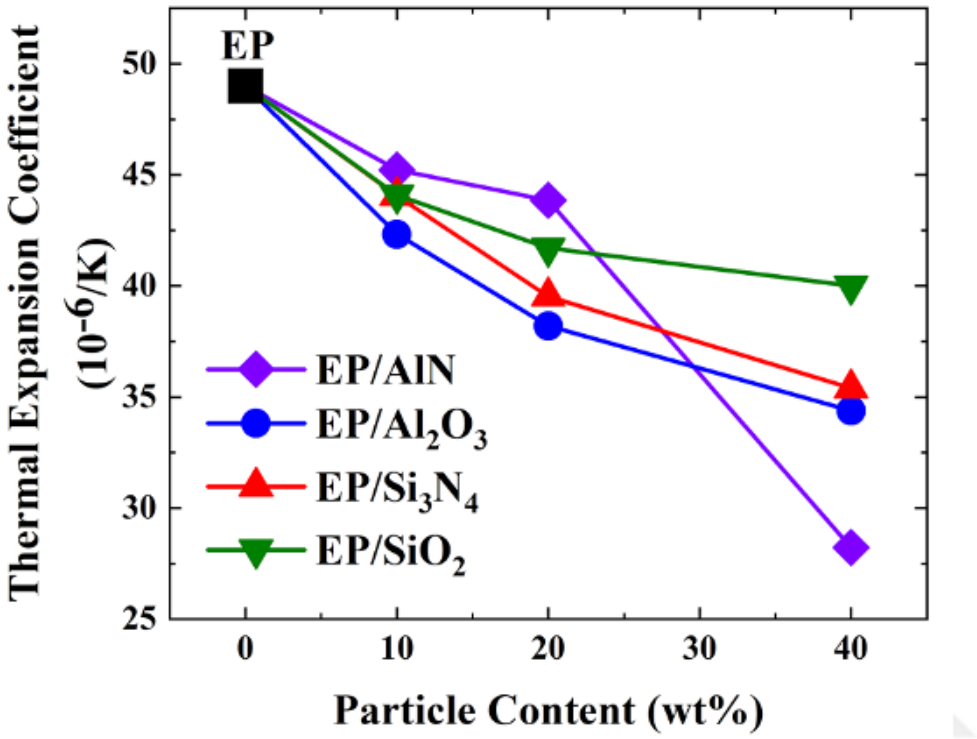

Figure 3.8. Effects of Particles on the Thermal Expansion Coefficient of Epoxy.

These significant decreases in the α values with increasing particle content can be at-tributed to the intrinsically much lower α values of ceramic particles leading to also mechanical constraints on the macromolecular structures of epoxy polymer, limiting its ability to undergo thermally induced segmental mobility required for volume expansion. This restriction against volume expansion becomes increasingly effective at higher particle contents, where particle–particle interactions and the formation of the mechanically constraining network become more pronounced. Although all filler systems exhibit a decreasing trend in thermal expansion coefficient with increasing particle content, nitride-based fillers, particularly 40 wt% AlN resulted in a more pronounced suppression effect compared to others. This behavior can be attributed to the inherently lower intrinsic α and higher elastic

modulus, which impose a stronger mechanical constraint on the polymer matrix and more effectively restrict thermally induced chain mobility. Similar behavior was also observed in other studies [34,37].

3.5 Effects of Particles on the λ/α Ratio

The ratio of λ/α can be considered as a useful indicator to evaluate the overall thermal performance of filled epoxy specimens for microelectronic applications. A high λ/α ratio implies that the material is capable of efficiently dissipating heat while maintaining dimensional stability under thermal loading. As presented in Table 3.2, the incorporation of ceramic fillers significantly increased the λ/α ratio compared when compared to the neat epoxy system.

The λ/α ratio of the neat epoxy was calculated as 3.06, whereas all particle filled systems exhibited substantially higher ratios, indicating simultaneous enhancement in heat transfer capability and suppression of thermal expansion. Among the investigated fillers, AlN particles demonstrated the most pronounced improvement, particularly at higher loading levels. EP/AlN 40 wt% specimen showed the highest λ/α ratio of 18.93, which can be attributed to the combined effect of relatively high intrinsic thermal conductivity of AlN and its ability to effectively restrict polymer chain mobility, thereby reducing the thermal expansion coefficient. In comparison, Si_3N_4 and Al_2O_3 filled systems also showed considerable improvements, with λ/α values reaching 16.00 and 15.00 at 40 wt% loading, respectively.

Although SiO_2 filled specimens exhibited high thermal conductivity values, their relatively higher thermal expansion coefficients resulted in slightly lower λ/α ratios

at high filler contents. These findings indicate that λ/α ratio provides a comprehensive parameter for comparing filler efficiency in thermally conductive polymer composites. In the context of microelectronic packaging materials, such as die attach adhesives, underfills, and encapsulation compounds, materials with higher λ/α ratios are particularly desirable since they can effectively dissipate heat while minimizing thermally induced mechanical stresses between dissimilar materials.

3.6 Effects of Particles on the Glass Transition Temperature

For the possible influences of nitride and oxide particles on the Glass Transition Temperature (T_g) of the epoxy system, DMA analyses from Room Temperature to 100°C were conducted for all specimen combinations to determine $tan\ \delta$ curves, which is the ratio of Loss Modulus to Storage Modulus. $Tan\ \delta$ curves obtained for each combination are shown in Figure 3.9. Then, values of the glass transition temperatures taken as the "peaks" of $tan\ \delta$ curves are evaluated in Figure 3.10 and tabulated in Table 3.2.

Peaks of the $tan\ \delta$ curves in Figure 3.9 and their values considered as T_g of the specimens in Figure 3.10 and Table 3.2 indicated that incorporation of nitride and oxide particles into the epoxy resin all resulted in certain degree of increases in the glass transition temperature of neat epoxy determined as 51°C. Although there were slight differences between each particle used; increases in the T_g values were more pronounced at higher particle loading. For example, when particles were added as 10 wt%; increases in the T_g values were up to 7°C; when 20 wt% particles were added increases were up to 12°C; similarly increases were up to 17°C when 40 wt% particles were added. In the literature [50,55] similar increases of T_g from 49°C to 51-58°C were cited after incorporating SiO_2 particles.

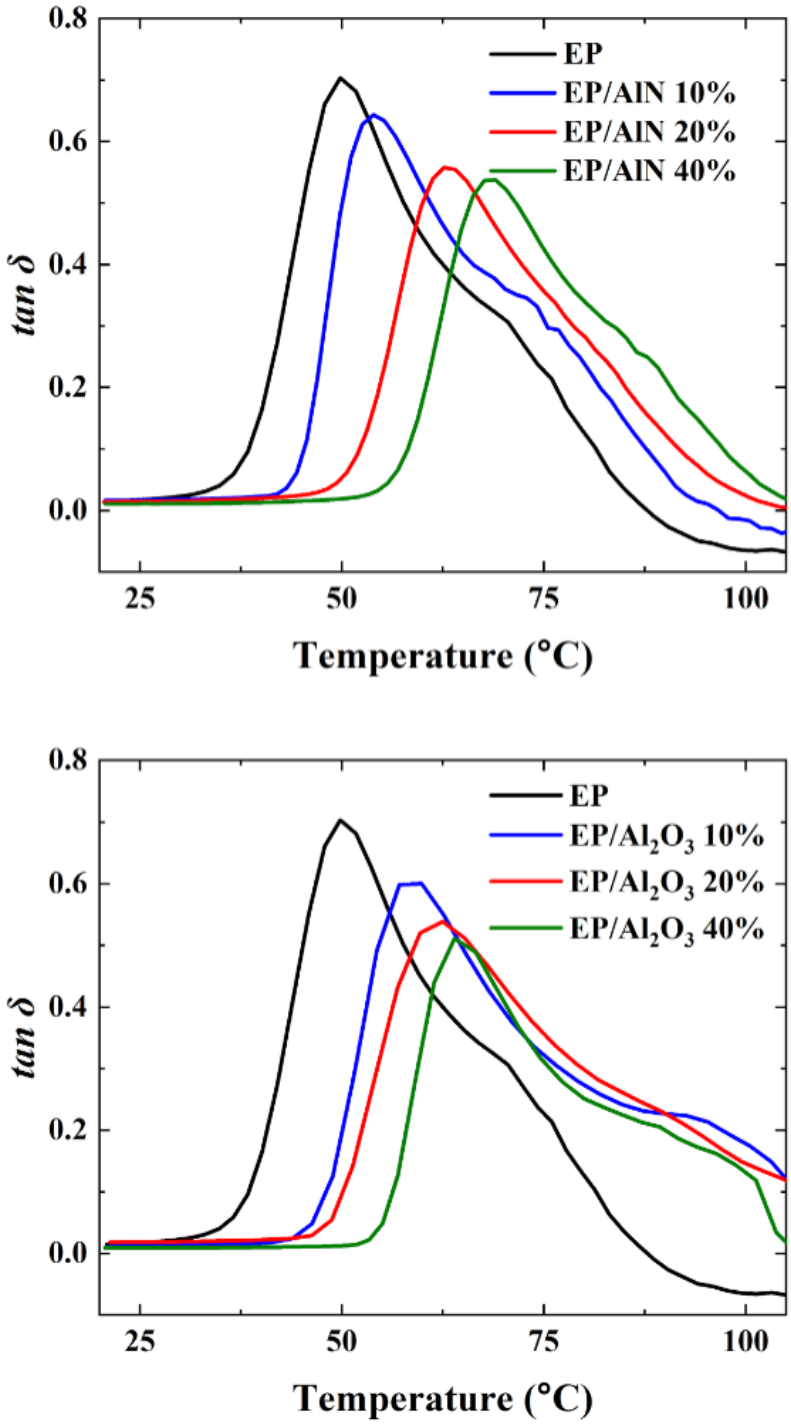

Figure 3.9. Effects of Particles on the *tan δ* curves of Epoxy determined by DMA.

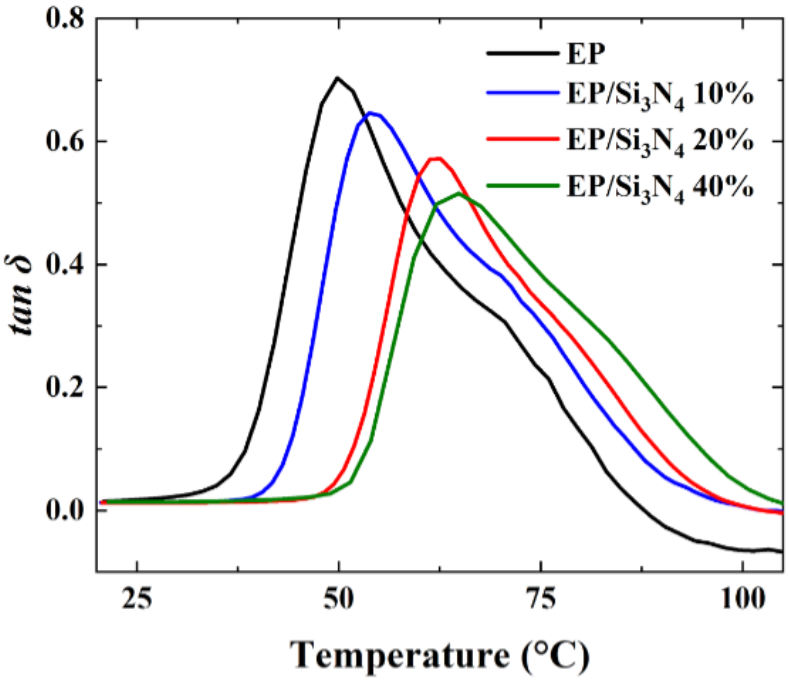

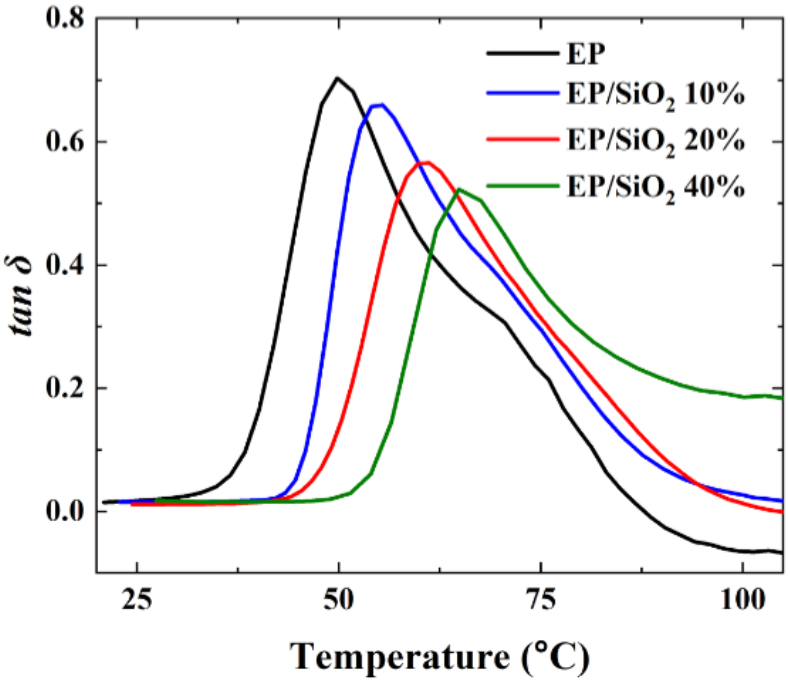

Figure 3.9. Continued.

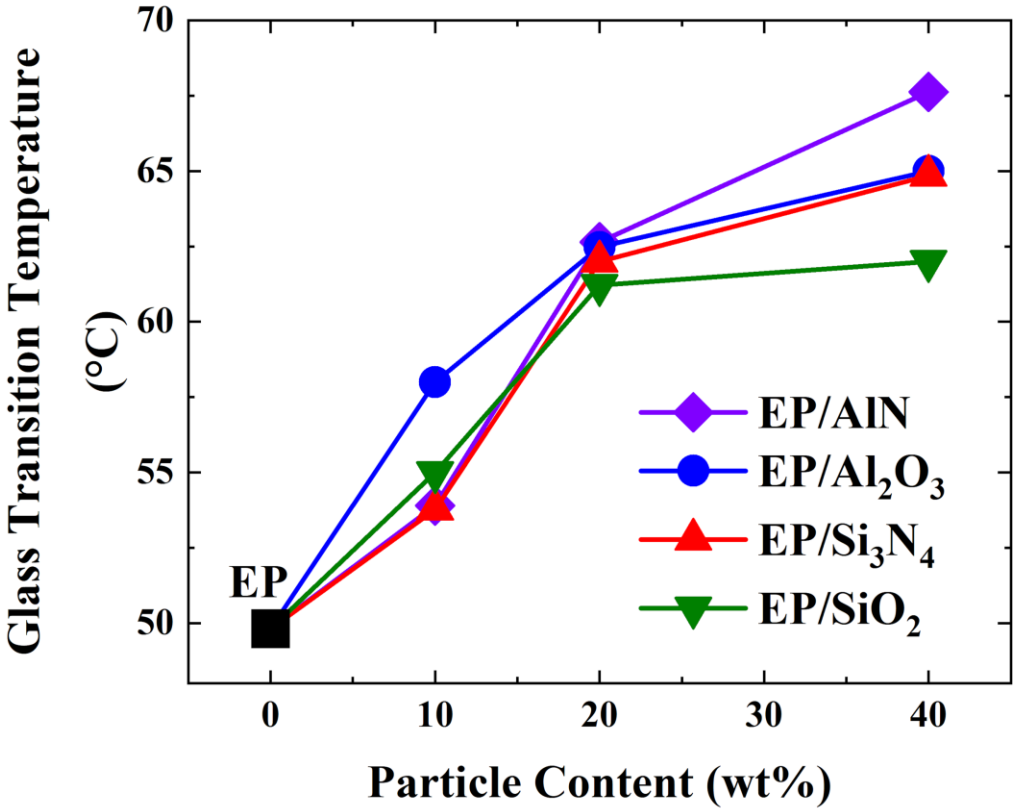

Figure 3.10. Effects of Particles on the Glass Transition Temperature of Epoxy.

It is known that *tan δ peaks* obtained by dynamic mechanical analysis is commonly associated with the *α-relaxation* process of the thermosetting epoxy network structure; and provides a reliable indication of T_g.

When the temperature rises to the T_g of the epoxy system, its mechanical rigidity including Storage Modulus drops significantly via the *α-relaxation* process depending mainly on the segmental mobility of the cross-linked epoxy network structure.

Therefore, addition of nitride and oxide particles resulted in shifting of *tan δ peaks* towards higher temperatures due to their restrictive actions on the segmental mobility of the neat epoxy structure. Of course, increasing the amount of particles lead to more segmental restriction resulting in higher Tg increases.

Apart from shifting in the *tan δ peaks* of the filled-epoxy specimens, Figure 3.9 also shows that there are significant decreases in their intensity and broadening, which might point out a limitation of segmental mobility and an increase in the heterogeneity of the network structure upon the introduction of fillers. Similarly Omrani *et al.* [53] reported that, this significant decrease in peak intensity and broadening indicates a wider distribution of relaxation times and increased microstructural heterogeneity.

Oxide surfaces (SiO_2 and Al_2O_3) tend to generate a more pronounced interphase (via polar surface groups and stronger secondary interactions), often leading to stronger broadening and high-temperature tailing that indicates a larger fraction of constrained polymer.

Nitride-filled systems (AlN and $Si_3\ N_4$), while still shifting T_g upward, can show comparatively different peak shapes depending on how effectively they disperse and interact with the matrix; in such cases, broadening is dominated more by physical barrier/confinement and microstructural heterogeneity rather than strong interfacial bonding.

3.7 Effects of Particles on the Thermal Degradation Temperature

In order to reveal effects of nitride and oxide particles on the Thermal Degradation Temperature (T_d) of the epoxy system, TGA analyses were conducted for neat and filled specimens. Thermogravimetric (TG) curves obtained for each combination are shown in. Note that in the insets of each group, Derivative Thermogravimetric (DTG) curves are also given. Then, DTG peaks representing the temperature for maximum weight losses are considered as the Thermal Degradation Temperature (T_d) of the specimens. Consequently, effects of the particles on the T_d values of epoxy are evaluated in Figure 3.12 and tabulated in Table 3.2.

Thermal degradation temperature (T_d) of each specimen group in Figure 3.11 and Table 3.2 revealed that addition of nitride and oxide particles into the epoxy resin all resulted in increases in the T_d of neat epoxy determined as 324°C. Although there were slight differences between each particle used; again increases in the T_d values were more pronounced at higher particle loading. For example, when particles were added as 10 wt%; increases in the T_d values were up to 11°C; when 20 wt% particles were added increases were up to 18°C; similarly increases were up to 32°C when 40 wt% particles were added. These rises in the T_d values reported in literature [50] were around 8–9°C.

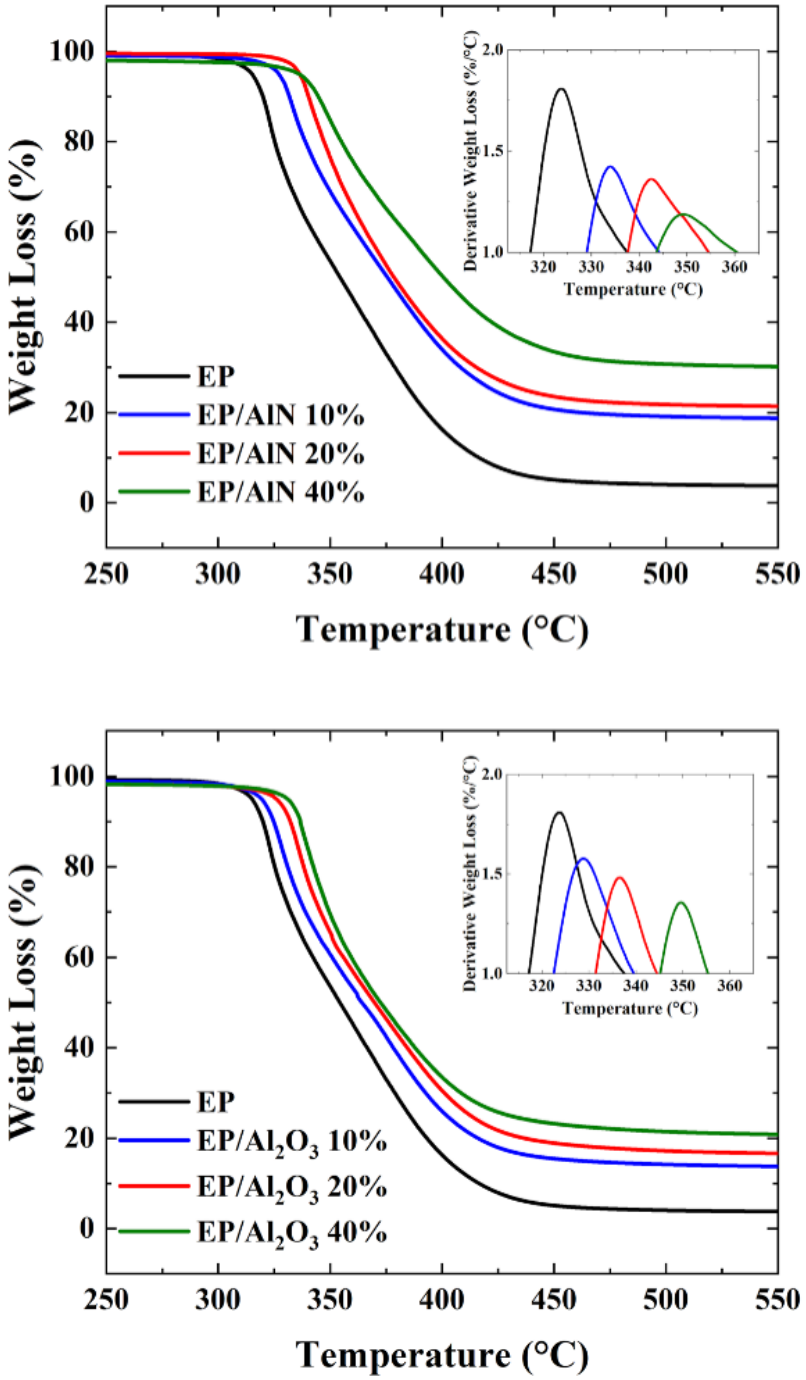

Figure 3.11. Effects of Particles on the Thermogravimetric (TG), and in the insets, Derivative Thermogravimetric (DTG) Curves of Epoxy.

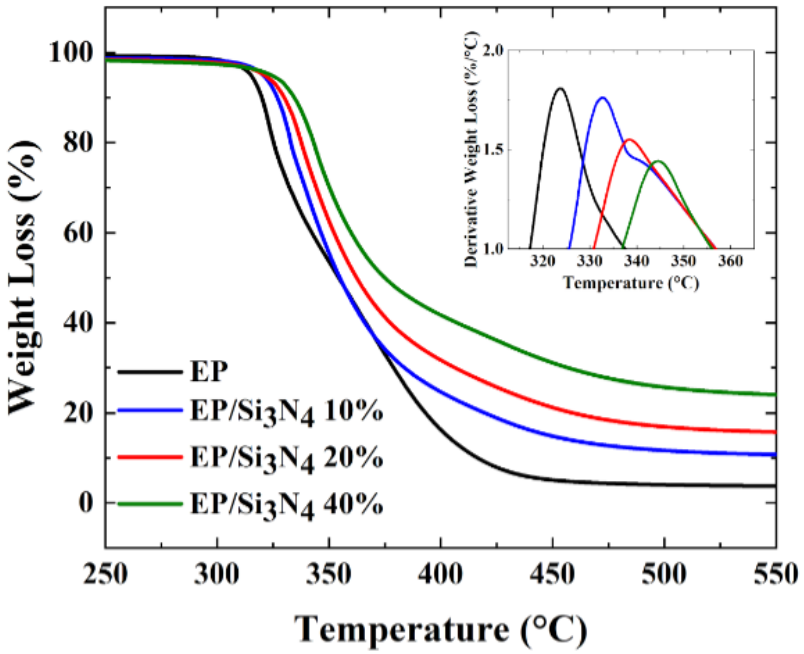

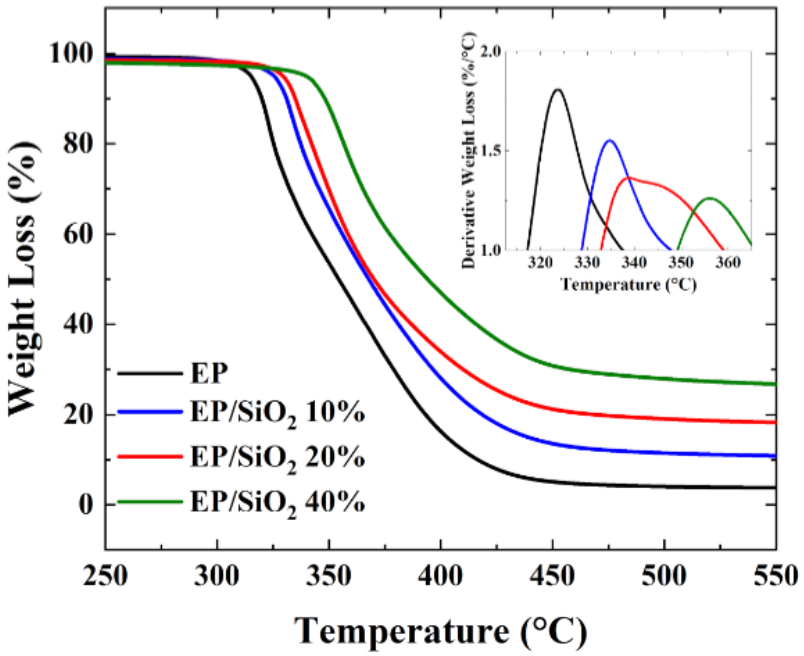

Figure 3.11. Continued.

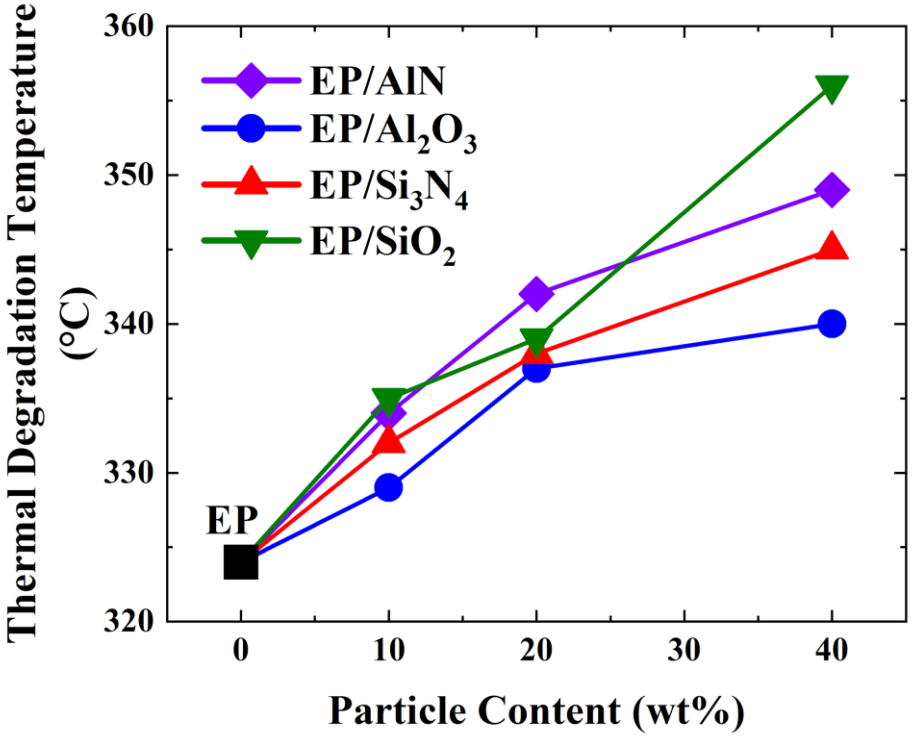

Figure 3.12. Effects of Particles on the Thermal Degradation Temperature of Epoxy.

It is known that thermal degradation of the epoxy structure takes place by the chemical deterioration and decomposition of the certain covalent bonds present in the cross-linked network structure.

Thus, these increases in the T_d values would be especially due to the heat barrier effects of the particles during thermal decomposition path of the epoxy. Because, compared to the epoxy; AlN, Al_2O_3, Si_3N_4 and SiO_2 particles all being *high-temperature ceramic materials* have much higher thermal stability (all of them higher than 1000°C) and shielding effect against transportation of heat and volatile products formed during thermal decomposition of the epoxy matrix.

Although filler loading is the dominant factor controlling thermal stability, particle chemistry and interfacial characteristics also influence resistance to degradation. Improved T_d values can be attributed to the barrier effect of inorganic particles, which restrict heat transfer within the matrix, delay volatile diffusion, and hinder chain scission reactions. Among the investigated systems, 40 wt% SiO_2 filled specimen resulted in highest stabilization, indicating a potentially stronger matrix–particle interaction, which can be linked to surface silanol groups, or more effective thermal shielding effect compared to the other ceramic fillers.

Table 3.2. Effects of Particles on the values of λ, α, λ/α, T_g and T_d of Epoxy.

	λ (W/m·K)	α (10^{-6}/K)	λ/α (W/10^{-9}·m)	T_g (°C)	T_d (°C)
EP	0.15	49	3.06	51	324
EP/AlN 10%	0.27	45	6.00	54	334
EP/AlN 20%	0.35	44	7.95	63	342
EP/AlN 40%	0.53	28	18.93	68	349
EP/Al_2O_3 10%	0.22	42	5.24	58	329
EP/Al_2O_3 20%	0.31	38	8.16	62	337
EP/Al_2O_3 40%	0.51	34	15.00	65	340
EP/Si_3N_4 10%	0.21	44	4.77	54	332
EP/Si_3N_4 20%	0.32	40	8.00	62	338
EP/Si_3N_4 40%	0.56	35	16.00	65	345
EP/SiO_2 10%	0.36	44	8.18	55	335
EP/SiO_2 20%	0.41	42	9.76	61	339
EP/SiO_2 40%	0.54	40	13.50	65	356

3.8 Effects of Particles on the Adhesion Strength

In microelectronic devices when epoxy resins are used, improving their thermal performance would be not sufficient, a certain degree of adhesion strength would be also necessary. Because in these applications epoxy resins were especially used as

“underfill” or “coating” materials. In order to observe effects of nitride and oxide particles on the degree of adhesion, results of Lap Shear Adhesion tests conducted for all specimen combinations are given in Figure 3.13.

It was observed that Lap Shear Adhesion Strength of the neat epoxy resin was 8 MPa, after the incorporation of all particles at all contents, no detrimental effects were seen, this means that adhesion strength of the neat epoxy resin could be maintained without any problem. In fact, use of particles increased adhesion strength values up to 12-13 MPa. These enhancements can be attributed to the reinforcement action of the particles leading to suppression of the epoxy matrix deformation under shear loading.

After each test, failure region of the specimen surfaces was carefully examined in order to determine whether their failure modes were “adhesive”, “cohesive”, or “mixed” (Figure 3.14). As shown in Figure 3.15, it was observed that majority of the specimens failed with a “mixed” mode.

In the literature it was reported [71] that when SiO_2 particles were used adhesion strength was 9-10 MPa. In the other studies [72–74] using other ceramic particles, they also observed mixed failure mode after their lap shear tests.

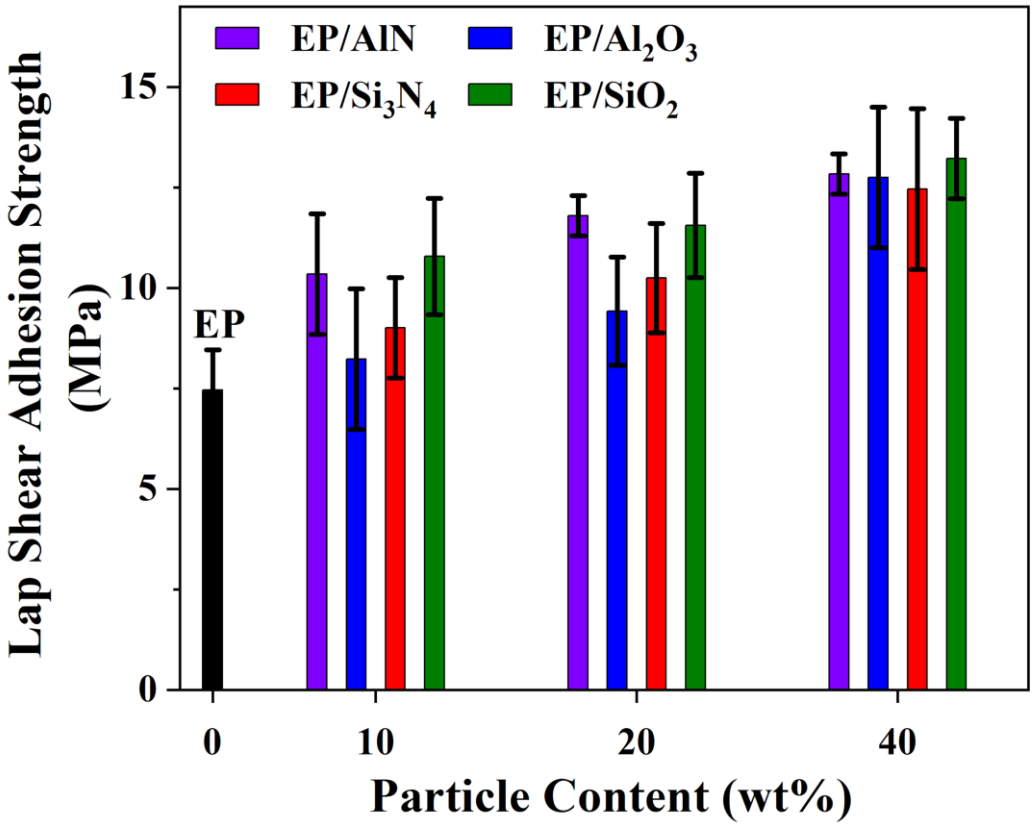

Figure 3.13. Effects of Particles on the Lap Shear Adhesion Strength of Epoxy.

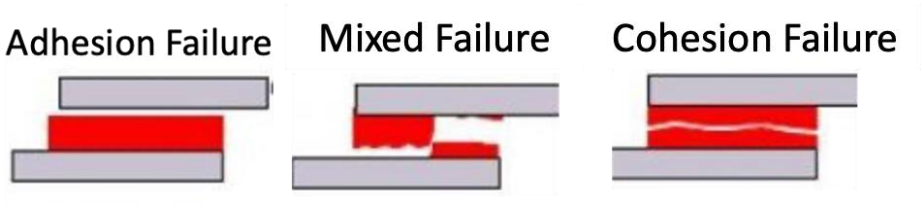

Figure 3.14. Failure modes of Lap Shear Test.



Figure 3.15. Examples of the "Mixed" Failure Mode observed after Lap Shear Tests.

3.9 Effects of Particles on the Storage Modulus

As discussed in Section 3.5 above, DMA analysis starting from Room Temperature to 100°C were conducted especially to determine *Tan Delta* curves for the evaluation of T_g values. In this final section, since influences of temperature on the mechanical performance of microelectronic parts could be critical; changes in the mechanical stiffness of the specimens were also evaluated by using the values of Storage Modulus (*E'*) at 25°C and 50°C.

Storage Modulus value of neat epoxy at 25°C was recorded as only 1.98 GPa. Figure 3.16 and Table 3.3 clearly indicated that after the incorporation of all particles at all contents, *E'* values at 25°C increased gradually parallel to the particle content. Of course, improvements were more significant (being almost 50% increase) when the

particle contents were 40 wt%. For instance, for the EP/SiO_2 40% specimen, *E'* value at 25°C increased up to 3.66 GPa.

These enhancements in the storage modulus values can be attributed to the two typical *stiffening mechanisms* observed in the polymer matrix composite materials. That is, "decrease in the mobility of matrix", and "efficient load transfer from the matrix" to intrinsically stronger and stiffer ceramic particles.

As expected, when the temperature was raised to 50°C, it was seen that *E'* value of neat epoxy almost diminished (being only 0.2 GPa). However, it was revealed that after the incorporation of all particles at all contents, *E'* values at 50°C increased again gradually parallel to the particle content. For all nitride and oxide particles, when their contents were 40 wt%; *E'* values at 50°C were all above 2 GPa.

Thus, it can be stated that, incorporation of nitride and oxide particles into epoxy would increase not only thermal performance of microelectronic parts but also they would keep mechanical rigidity of the devices at least up to 50°C.

Table 3.3. Effects of Particles on the values of Storage Modulus (*E'*) of Epoxy at 25°C and 50°C.

	***E'* at 25°C (GPa)**	***E'* at 50°C (GPa)**
EP	1.98	0.20
EP/AlN 10%	2.35	0.94
EP/AlN 20%	2.37	1.67
EP/AlN 40%	2.63	2.01
EP/Al_2O_3 10%	2.51	1.78
EP/Al_2O_3 20%	2.54	1.83
EP/Al_2O_3 40%	2.82	2.29
EP/Si_3N_4 10%	2.33	0.98
EP/Si_3N_4 20%	2.48	1.50
EP/Si_3N_4 40%	2.87	2.05
EP/SiO_2 10%	2.23	1.36
EP/SiO_2 20%	2.36	1.43
EP/SiO_2 40%	3.66	2.13

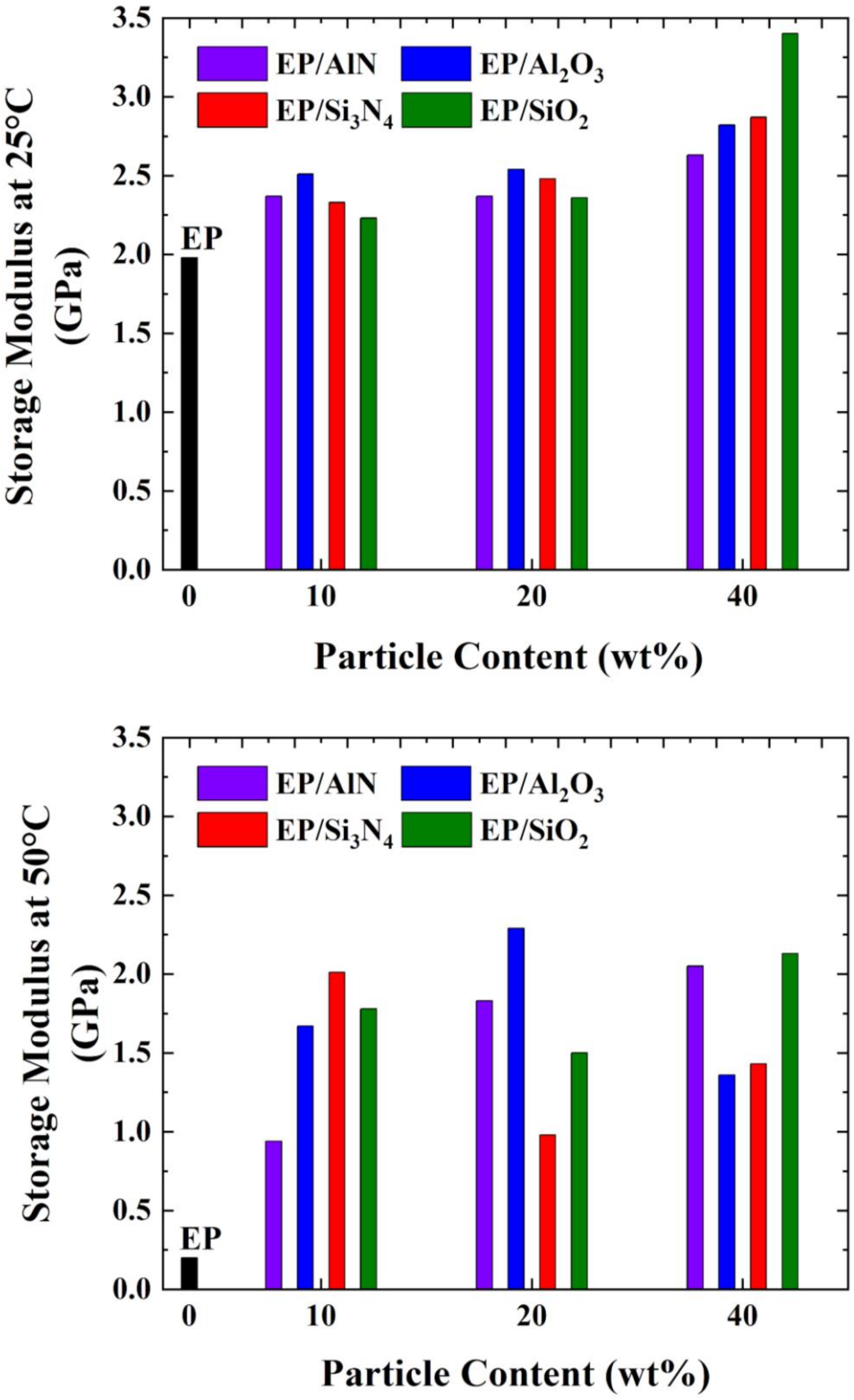

Figure 3.16. Effects of Particles on the Storage Modulus of Epoxy.

3.10 Relevance of the Results to Microelectronic Applications

The improvements in the thermal and mechanical properties of the particle filled epoxy systems observed in this study indicate that these materials have strong potential for use in several microelectronic packaging applications. Microelectronic devices generate significant heat during operation and efficient heat dissipation is essential to maintain reliability and prevent thermal failure. The incorporation of oxide and nitride particles increased the thermal conductivity of the epoxy resin by more than three times compared to the neat epoxy system, which can significantly enhance heat transfer away from active semiconductor components. This improvement is particularly beneficial for die bonding adhesives and underfill materials, where the adhesive layer directly participates in the thermal management of the interfaces.

Another critical issue in microelectronic packaging is the mismatch in thermal expansion coefficients between different materials such as silicon chips, metallic lead frames and polymeric encapsulants. The significant reduction in the thermal expansion coefficient of the epoxy system with increasing particle content helps to minimize thermally induced stresses during heating and cooling cycles. Such a reduction in thermal strain mismatch is particularly advantageous for underfill and glob top encapsulation applications, where dimensional stability is required to maintain the integrity of solder joints and wire bonds.

In addition to thermal expansion control, the observed increase in Glass Transition Temperature improves the thermal stability of the epoxy matrix during device operation. Higher T_g values ensure that the polymer network remains in a mechanically stable glassy state over a wider temperature range, which is critical for conformal coating and encapsulation materials exposed to elevated service

temperatures. The improved thermal degradation temperature further supports the use of these filled epoxy systems in applications where long-term thermal reliability is required.

From a mechanical perspective, the increase in storage modulus at both 25°C and 50°C demonstrates that particle incorporation significantly enhances the rigidity of the epoxy network. Maintaining sufficient mechanical stiffness is particularly important in potting and sealing applications, where encapsulated components must resist mechanical deformation while simultaneously protecting sensitive electronic parts.

Finally, the results of the lap shear adhesion tests revealed that the addition of nitride and oxide particles did not compromise the adhesion strength of the epoxy system. In fact, slight improvements in adhesion were observed. This indicates that the incorporation of ceramic particles can enhance thermal and mechanical performance without sacrificing the adhesive functionality required in many microelectronic packaging applications.

Overall, the combined improvements in thermal conductivity, thermal expansion behavior, thermal stability, mechanical rigidity, and adhesion strength suggest that oxide- and nitride-filled epoxy systems can provide a balanced property profile suitable for advanced microelectronic device packaging.

CHAPTER 4

CONCLUSIONS AND FUTURE RECOMMENDATIONS

4.1 Conclusions

Main conclusions on the effects of 10, 20, 40 wt% micron-sized particles (aluminum nitride, aluminum oxide, silicon nitride, silicon oxide) in terms of especially thermal performance of the epoxy resin used in microelectronic devices can be summarized as follows.

- Thermal Conductivity was identified as the most critical parameter governing the heat dissipation capability of epoxy components in microelectronic assemblies. The incorporation of filler particles progressively enhanced λ, increasing it from 0.15 W/m·K for neat epoxy to more than three times this value at 40 wt% loading. This improvement can be attributed to the formation of certain conductive pathways within the polymer matrix and reduced phonon scattering due to the presence of high conductivity ceramic phases. Although minor differences were observed among particle types, filler loading was the dominant factor controlling thermal transport behavior.

- A significant reduction in Thermal Expansion Coefficient was achieved with increasing filler content, decreasing from 49×10^{-6} /K for neat epoxy to approximately 28×10^{-6} /K at 40 wt%, corresponding to a 43% reduction. This decrease is primarily associated with the inherently low α values of fillers and the restriction of polymer chain mobility at the particle–matrix interface. The reduced thermal expansion mismatch is particularly beneficial for minimizing thermomechanical stresses and improving dimensional

stability in microelectronic structures where “thermal strain mismatch” is a critical issue between dissimilar materials.

- The λ/α ratio was identified as a comprehensive indicator of thermal performance, demonstrating that ceramic filler incorporation, particularly 40 wt% AlN, significantly enhances heat dissipation while suppressing thermal expansion, making AlN filled epoxy systems the most effective candidates for dimensionally stable and thermally efficient microelectronic packaging applications.

- All investigated nitride and oxide fillers contributed to an increase in T_g, from 51°C for neat epoxy to up to 68°C at higher loadings. The elevation in T_g suggests enhanced interfacial interactions and reduced segmental mobility of the polymer macromolecules. This improvement indicates improved thermal reliability under service conditions approaching elevated operating temperatures.

- The addition of nitride and oxide particles also resulted in increased thermal degradation resistance, raising T_d from 324°C to approximately 356°C at 40 wt% filler loading. This enhancement can be attributed to the barrier effect of dispersed particles, which delay volatile product diffusion and limit thermal decomposition mechanism. Improved thermal stability further supports the suitability of these composites for high temperature microelectronic applications.

- Moreover, lap shear adhesion tests revealed that there was no decrease in the adhesion strength of the neat epoxy after the incorporation of all particles at all contents; with slight increases from 8 MPa to 12-13 MPa. Thus, it can be stated that apart from substantial improvements in thermal properties, no detrimental effects on adhesive performance were observed. The preservation

of adhesion strength indicates that the incorporation of micron-sized fillers does not compromise interfacial bonding capability, which is essential for maintaining structural integrity in bonded microelectronic assemblies.

- Additionally, incorporation of all particles revealed that Storage Modulus value of neat epoxy at 25°C could be increased from only 1.98 GPa up to 3.66 GPa; while at 50°C almost diminished *E'* value (0.2 GPa) of neat epoxy could be maintained above 2 GPa. Therefore, it could be interpreted that, nitride and oxide filled epoxy would improve not only thermal performance of microelectronic parts but also they would keep mechanical rigidity of the devices at least up to 50°C.

Overall, these conclusions demonstrate that optimizing filler loading enables simultaneous enhancement of thermal conductivity, dimensional stability, and thermal resistance while maintaining adequate adhesion performance and mechanical rigidity. Such balanced property improvement is critical for the long-term reliability of epoxy based components in advanced microelectronic devices.

4.2 Future Recommendations

While the present study focused on the incorporation of micron sized AlN, Al_2O_3 , Si_3N_4 , and SiO_2 particles into epoxy matrix, future research should primarily investigate hybrid filler systems to further enhance thermal performance without excessively increasing filler loading. The synergistic combination of micro- and nano-sized particles, or the integration of fillers with complementary intrinsic thermal conductivities and morphologies, may significantly improve particle packing density and promote the formation of more efficient heat conduction networks within the epoxy matrix. Such hybrid architectures could reduce interfacial thermal resistance and phonon scattering, thereby achieving higher thermal

conductivity at lower overall filler content while maintaining acceptable viscosity and processability for microelectronic packaging applications.

Moreover, systematic studies examining the optimal hybrid ratios, particle size distributions, and surface functionalization strategies are recommended to maximize filler–matrix interfacial compatibility and dispersion homogeneity. The influence of hybrid systems on curing behaviour, glass transition temperature, storage modulus, and coefficient of thermal expansion should also be evaluated to determine potential trade-offs between thermal transport and thermo-mechanical stability. In addition, advanced microstructural characterization and numerical modeling approaches could be employed to elucidate heat transfer pathways and establish quantitative structure–property relationships. Such investigations would contribute to the rational design of next-generation high-thermal-conductivity epoxy composites tailored for demanding microelectronic device applications.

REFERENCES

1. Ellis, B. *Chemistry and Technology of Epoxy Resins*; First.; Springer Dordrecht, 1993; ISBN 978-0-7514-0095-3.

2. Grovenor, C.R.M. *Microelectronic Materials*; Taylor & Francis Group: Great Britain, 1998;

3. Ng, F.C.; Abas, M.A. Underfill Flow in Flip-Chip Encapsulation Process: A Review. *J. Electron. Packag.* **2022**, *144*, doi:https://doi.org/10.1115/1.4050697.

4. Ardebili, H.; Zhang, J.; Pecht, M.G. *Encapsulation Technologies for Electronic Applications*; Second Edition.; Elsevier Inc., 2018; ISBN 978-0-12-811978-5.

5. Toleno, B.J. Conformal Coatings. In *Lead-free Soldering Process Development and Reliability*; John Wiley & Sons, Inc, 2020; pp. 429–465 ISBN 978-1-119-48203-1.

6. Kinjo, N.; Ogata, M.; Nishi, K.; Kaneda, A.; Dusek, K. Epoxy Molding Compounds as Encapsulation Materials for Microelectronic Devices.; Springer Berlin Heidelberg, 1989; Vol. 88.

7. Bonding Materials | WeldTone Available online: http://en.weldtone.com/products/bonding-materials (accessed on 16 February 2026).

8. Glob Top Sealing Compounds - Hoenle 2025.

9. MorePCBAb PCB Conformal Coating for PCB Protection. *MorePCB* 2023.

10. Low Shrinkage Epoxy | 9803 Epoxy with Very Low Shrinkage. *Unmanned Syst. Technol.*

11. Low Temperature Cure BGA Flip Chip Underfill PCB Epoxy Process Adhesive Glue Material Manufacturers | High Temperature-Resistant Underfill Material Supppliers. *Epoxy Adhes. Glue Manuf.*

12. Menczel, J.D.; Prime, R.B. *Thermal Analysis of Polymers*; John Wiley & Sons, Inc., 2009;

13. Wagner, M. *Thermal Analysis in Practise*; 1st Edition.; 2017; ISBN 978-1-56990-643-9.

14. Ma, A.; Chen, W.; Hou, Y.; Zhang, G. The Preparation and Cure Kinetics Researches of Thermal Conductivity Epoxy/AlN Composites. *Polym.-Plast. Technol. Eng.* **2010**, *49*, 354–358, doi:10.1080/03602550903532091.

15. Hutchinson, J.M.; Roman, F.; Cortes, P.; Calventus, Y. Epoxy Composites Filled with Boron Nitride and Aluminum Nitride for Improved Thermal Conductivity. *Polimery* **2017**, *62*, 560–566, doi:10.14314/polimery.2017.560.

16. Sanctuary, R.; Baller, J.; Zielinski, B.; Becker, N.; Krüger, J.K.; Philipp, M.; Müller, U.; Ziehmer, M. Influence of Al2O3 Nanoparticles on the Isothermal Cure of an Epoxy Resin. *J. Phys. Condens. Matter* **2009**, *21*, 035118, doi:10.1088/0953-8984/21/3/035118.

17. Yang, C.-F.; Wang, L.-F.; Wu, S.-M.; Su, C.-C. Characterization and Curing Kinetics of Epoxy/Silica Nano-Hybrids. *Materials* **2015**, *8*, 7032–7040, doi:10.3390/ma8105357.

18. Chen, X.; Dai, C.; Jiang, T.; Paramane, A. Enhanced Thermal and Dielectric Performance of Epoxy Resin/Aluminum Nitride Nanocomposites at High Temperatures. *Polym. Compos.* **2020**, *41*, 5375–5386, doi:10.1002/pc.25802.

19. Kim, W.; Bae, J.; Choi, I.; Kim, Y. Thermally Conductive EMC (Epoxy Molding Compound) for Microelectronic Encapsulation. *Polym. Eng. Sci.* **1999**, *39*, 756–766, doi:10.1002/pen.11464.

20. Konzelmann, S.; Hoffmann, C.; Merte, R.; Peier, D. Thermal and Electrical Properties of Aluminum Nitride Filled Epoxy-Resin Compound. *IEEE Trans. Dielectr. Electr. Insul.* **2008**, *15*, 327–333, doi:10.1109/TDEI.2008.4483449.

21. Nagai, Y.; Lai, G.-C. Thermal Conductivity of Epoxy Resin Filled with Particulate Aluminum Nitride Powder. *J. Ceram. Soc. Jpn.* **1997**, *105*, 197–200, doi:10.2109/jcersj.105.197.

22. Khan, A.; Puttegowda, M.; Jagadeesh, P.; Marwani, H.M.; Asiri, A.M.; Manikandan, A.; Parwaz Khan, A.A.; Ashraf, G.M.; Rangappa, S.M.; Siengchin, S. Review on Nitride Compounds and Its Polymer Composites: A Multifunctional Material. *J. Mater. Res. Technol.* **2022**, *18*, 2175–2193, doi:10.1016/j.jmrt.2022.03.032.

23. Lee Sanchez, W.A.; Huang, C.-Y.; Chen, J.-X.; Soong, Y.-C.; Chan, Y.-N.; Chiou, K.-C.; Lee, T.-M.; Cheng, C.-C.; Chiu, C.-W. Enhanced Thermal Conductivity of Epoxy Composites Filled with Al2O3/Boron Nitride Hybrids for Underfill Encapsulation Materials. *Polymers* **2021**, *13*, 147, doi:10.3390/polym13010147.

24. Zhao, Y.; Zhai, Z.; Drummer, D. Thermal Conductivity of Aluminosilicate- and Aluminum Oxide-Filled Thermosets for Injection Molding: Effect of Filler Content, Filler Size and Filler Geometry. *Polymers* **2018**, *10*, 457, doi:10.3390/polym10040457.

25. Agrawal, A.; Satapathy, A. Thermal and Dielectric Behavior of Epoxy Composites Filled with Ceramic Micro Particulates. *J. Compos. Mater.* **2014**, *48*, 3755–3769, doi:10.1177/0021998313513205.

26. Fu, Y.-X.; He, Z.-X.; Mo, D.-C.; Lu, S.-S. Thermal Conductivity Enhancement with Different Fillers for Epoxy Resin Adhesives. *Appl. Therm. Eng.* **2014**, *66*, 493–498, doi:10.1016/j.applthermaleng.2014.02.044.

27. Hu, Y.; Du, G.; Chen, N. A Novel Approach for Al2O3/Epoxy Composites with High Strength and Thermal Conductivity. *Compos. Sci. Technol.* **2016**, *124*, 36–43, doi:10.1016/j.compscitech.2016.01.010.

28. Li, H.; Zheng, W. Enhanced Thermal Conductivity of Epoxy/Alumina Composite through Multiscale-Disperse Packing. *J. Compos. Mater.* **2021**, *55*, 17–25, doi:10.1177/0021998320942575.

29. Moreira, D.C.; Braga, N.R.; Sphaier, L.A.; Nunes, L.C. Size Effect on the Thermal Intensification of Alumina-Filled Nanocomposites. *J. Compos. Mater.* **2016**, *50*, 3699–3707, doi:10.1177/0021998315624253.

30. Tang, Y.; Ge, G.; Li, Y.; Huang, L. Effect of Al2O3 with Different Nanostructures on the Insulating Properties of Epoxy-Based Composites. *Materials* **2020**, *13*, 4235, doi:10.3390/ma13194235.

31. Liang, M.; Wong, K.L. Study of Mechanical and Thermal Performances of Epoxy Resin Filled with Micro Particles and Nanoparticles. *Energy Procedia* **2017**, *110*, 156–161, doi:10.1016/j.egypro.2017.03.121.

32. Kusunose, T.; Yagi, T.; Firoz, S.H.; Sekino, T. Fabrication of Epoxy/Silicon Nitride Nanowire Composites and Evaluation of Their Thermal Conductivity. *J. Mater. Chem. A* **2013**, *1*, 3440, doi:10.1039/c3ta00686g.

33. Voo, R.; Mariatti, M.; Sim, L.C. Thermal Properties and Moisture Absorption of Nanofillers- filled Epoxy Composite Thin Film for Electronic Application. *Polym. Adv. Technol.* **2012**, *23*, 1620–1627, doi:10.1002/pat.3039.

34. Duwe, S.; Arlt, C.; Aranda, S.; Riedel, U.; Ziegmann, G. A Detailed Thermal Analysis of Nanocomposites Filled with SiO2, AlN or Boehmite at Varied Contents and a Review of Selected Rules of Mixture. *Compos. Sci. Technol.* **2012**, *72*, 1324–1330, doi:10.1016/j.compscitech.2012.04.015.

35. Vo, H.T.; Todd, M.; Shi, F.G.; Shapiro, A.A.; Edwards, M. Towards Model-Based Engineering of Underfill Materials: CTE Modeling. *Microelectron. J.* **2021**, 331–338.

36. McGrath, L.M.; Parnas, R.S.; King, S.H.; Schroeder, J.L.; Fischer, D.A.; Lenhart, J.L. Investigation of the Thermal, Mechanical, and Fracture Properties of Alumina–Epoxy Composites. *Polymer* **2008**, *49*, 999–1014, doi:10.1016/j.polymer.2007.12.014.

37. Jiang, W.; Jin, F.-L.; Park, S.-J. Thermo-Mechanical Behaviors of Epoxy Resins Reinforced with Nano-Al2O3 Particles. *J. Ind. Eng. Chem.* **2012**, *18*, 594–596, doi:10.1016/j.jiec.2011.11.140.

38. Hussain, M.; Nakahira, A.; Nishijima, S.; Niihara, K. Effects of Ceramic Particle Addition on the Thermal Contraction of Epoxy Materials at Cryogenic Temperature. *Key Eng. Mater.* **1998**, *161–163*, 363–370, doi:10.4028/www.scientific.net/KEM.161-163.363.

39. Vaisakh, S.S.; Hassanzadeh, M.; Metz, R.; Ramakrishnan, S.; Chappelle, D.; Sudha, J.D.; Ananthakumar, S. Effect of Nano/Micro-Mixed Ceramic Fillers on the Dielectric and Thermal Properties of Epoxy Polymer Composites: Dielectric and Thermal Properties of Epoxy-Ceramic Filler Composites. *Polym. Adv. Technol.* **2014**, *25*, 240–248, doi:10.1002/pat.3230.

40. Zeng, J.; Fu, R.; Shen, Y.; He, H.; Song, X. High Thermal Conductive Epoxy Molding Compound with Thermal Conductive Pathway. *J. Appl. Polym. Sci.* **2009**, *113*, 2117–2125, doi:10.1002/app.30045.

41. Ahmad, Z.; Al-Sagheer, F. Novel Epoxy–Silica Nano-Composites Using Epoxy-Modified Silica Hyper-Branched Structure. *Prog. Org. Coat.* **2015**, *80*, 65–70, doi:10.1016/j.porgcoat.2014.11.016.

42. An, H.; Liu, Z.; Tian, Q.; Li, J.; Zhou, C.; Liu, X.; Zhu, W. Thermal Behaviors of Nanoparticle Reinforced Epoxy Resins for Microelectronics Packaging. *Microelectron. Reliab.* **2019**, *93*, 39–44, doi:10.1016/j.microrel.2019.01.002.

43. Bujard, P.; Ansermet, J.P. Thermally Conductive Aluminium Nitride-Filled Epoxy Resin (for Electronic Packaging). In Proceedings of the Fifth Annual IEEE Semiconductor Thermal and Temperature Measurement Symposium; IEEE: San Diego, CA, USA, 1989; pp. 126–130.

44. Dai, C.; Chen, X.; Jiang, T.; Paramane, A.; Tanaka, Y. Improvement of Electrical and Material Properties of Epoxy Resin/ Aluminum Nitride Nanocomposites for Packaging Materials. *Polym. Test.* **2020**, *86*, 106502, doi:10.1016/j.polymertesting.2020.106502.

45. Perminov, V.P.; Modyanova, A.G.; Ryabkov, Y.I.; Sevbo, O.A.; Gailyunas, I.A.; Kuchin, A.V. Epoxy Composites Modified with Finely Dispersed Fillers. *Russ. J. Appl. Chem.* **2002**, *75*.

46. De Souza, J.P.B.; Reis, J.M.L.D. A Thermomechanical and Adhesion Analysis of Epoxy/Al2O3 Nanocomposites. *Nanomater. Nanotechnol.* **2015**, *5*, 18, doi:10.5772/60938.

47. Qiang, D.; Wang, X.; Wang, Y.; Andritsch, T.; Chen, G. Thermal Stability of Epoxy Nanocomposites: Surface Treatment and Morphology Impact Based on Nano SiO_2 and hBN Fillers. *Mater. Res. Express* **2019**, *6*, 105350, doi:10.1088/2053-1591/ab3f8f.

48. Ou, C.-F.; Shiu, M.-C. Preparation and Characterisation of Epoxy Composites Filled with Silica Nanoparticles. *Polym. Polym. Compos.* **2008**, *16*, 465–469, doi:10.1177/096739110801600708.

49. Tarrío-Saavedra, J.; López-Beceiro, J.; Naya, S.; Artiaga, R. Effect of Silica Content on Thermal Stability of Fumed Silica/Epoxy Composites. *Polym.*

Degrad. Stab. **2008**, *93*, 2133–2137, doi:10.1016/j.polymdegradstab.2008.08.006.

50. Allahverdi, A.; Ehsani, M.; Janpour, H.; Ahmadi, S. The Effect of Nanosilica on Mechanical, Thermal and Morphological Properties of Epoxy Coating. *Prog. Org. Coat.* **2012**, *75*, 543–548, doi:10.1016/j.porgcoat.2012.05.013.

51. Hiremath, V.; Singh, M.; Shukla, D.K. Effect of Post Curing Temperature on Viscoelastic and Flexural Properties of Epoxy/Alumina Polymer Nanocomposites. *Procedia Eng.* **2014**, *97*, 479–487, doi:10.1016/j.proeng.2014.12.272.

52. Naous, W.; Yu, X.; Zhang, Q.; Naito, K.; Kagawa, Y. Morphology, Tensile Properties, and Fracture Toughness of Epoxy/Al_2 O_3 Nanocomposites. *J. Polym. Sci. Part B Polym. Phys.* **2006**, *44*, 1466–1473, doi:10.1002/polb.20800.

53. Omrani, A.; Simon, L.C.; Rostami, A.A. The Effects of Alumina Nanoparticle on the Properties of an Epoxy Resin System. *Mater. Chem. Phys.* **2009**, *114*, 145–150, doi:10.1016/j.matchemphys.2008.08.090.

54. Simunin, M.M.; Voronin, A.S.; Fadeev, Yu.V.; Dobrosmyslov, S.S.; Kuular, A.A.; Shalygina, T.A.; Shabanova, K.A.; Chirkov, D.Yu.; Voronina, S.Yu.; Khartov, S.V. Influence of the Addition of Alumina Nanofibers on the Strength of Epoxy Resins. *Materials* **2023**, *16*, 1343, doi:10.3390/ma16041343.

55. Yao, X.F.; Yeh, H.Y.; Zhou, D.; Zhang, Y.H. The Structural Characterization and Properties of SiO2-Epoxy Nanocomposites. *J. Compos. Mater.* **2006**, *40*, 371–381, doi:10.1177/0021998305055193.

56. Aziz, T.; Mehmood, S.; Haq, F.; Ullah, R.; Khan, F.U.; Ullah, B.; Raheel, M.; Iqbal, M.; Ullah, A. Synthesis and Modification of Silica- based Epoxy Nanocomposites with Different Sol–Gel Process Enhanced Thermal and Mechanical Properties. *J. Appl. Polym. Sci.* **2021**, *138*, 51191, doi:10.1002/app.51191.

57. Lim, W.Y.L.; Jaafar, M.; Ishak, K.M.K.; Chinniah, K.; Chan, W.K. Thermo-mechanical Properties of Epoxy Composites Filled with Inorganic Particulate Fillers for Robust Solder Mask Application. *Polym. Int.* **2024**, *73*, 779–788, doi:10.1002/pi.6648.

58. Rashid, E.S.A.; Akil, H.M.; Ariffin, K.; Kooi, C.C. The Mechanical and Thermal Properties of Alumina Filled Epoxy. In Proceedings of the 2006 Thirty-First IEEE/CPMT International Electronics Manufacturing Technology Symposium; IEEE: Petaling Jaya, Malaysia, November 2006; pp. 282–287.

59. ASTM Internation. *Standard Test Method for Evaluating the Resistance to Thermal Transmission by the Guarded Heat Flow Meter Technique*; ASTM E1530-19; **2025**.

60. ASTM International. *Standard Test Method for Linear Thermal Expansion of Solid Materials With a Push-Rod Dilatometer*; ASTM E228-17;

61. ASTM International. *Standard Test Method for Apparent Shear Strength of Single-Lap-Joint Adhesively Bonded Metal Specimens by Tension Loading*; ASTM D1002-10;

62. Bekeshev, A.; Mostovoy, A.; Shcherbakov, A.; Tastanova, L.; Akhmetova, M.; Apendina, A.; Orynbassar, R.; Lopukhova, M. The Influence of Pristine and Aminoacetic Acid-Treated Aluminum Nitride on the Structure, Curing Processes, and Properties of Epoxy Nanocomposites. *J. Compos. Sci.* **2023**, *7*, 482, doi:10.3390/jcs7120482.

63. Gao, N.K.; Xu, Z.; Wu, C.; Li, R.H.; Jin, H.Y. Dispersion and Impact Strength of Epoxy Resin/Nano-Al_2O_3 Composites. *Mater. Sci. Forum* **2013**, *761*, 161–164, doi:10.4028/www.scientific.net/MSF.761.161.

64. Zheng, J.; Zhang, X.; Cao, J.; Chen, R.; Aziz, T.; Fan, H.; Bittencourt, C. Behavior of Epoxy Resin Filled with nano- SiO2 Treated with a Eugenol Epoxy Silane. *J. Appl. Polym. Sci.* **2021**, *138*, 50138, doi:10.1002/app.50138.

65. Kim, K.-M.; Kim, H.; Kim, H.-J. Enhancing Thermo-Mechanical Properties of Epoxy Composites Using Fumed Silica with Different Surface Treatment. *Polymers* **2021**, *13*, 2691, doi:10.3390/polym13162691.

66. Tang, J.; Chen, K.X.; Fu, C.S. Preparation and Properties of β-Si_3N_4/Epoxy Matrix Composite. *Key Eng. Mater.* **2007**, *336–338*, 1350–1352, doi:10.4028/www.scientific.net/KEM.336-338.1350.

67. Li, G.; He, Y.; Zhu, P.; Zhao, T.; Sun, R.; Lu, D.; Wong, C. Tailored Surface Chemistry of SiO2 Particles with Improved Rheological, Thermal-Mechanical and Adhesive Properties of Epoxy Based Composites for Underfill

Applications. *Polymer* **2018**, *156*, 111–120, doi:10.1016/j.polymer.2018.09.063.

68. Shimamura, A.; Hotta, Y.; Hyuga, H.; Kondo, N.; Hirao, K. Effect of Amounts and Types of Silicon Nitride on Thermal Conductivity of Si_3N_4/Epoxy Resin Composite. *J. Ceram. Soc. Jpn.* **2015**, *123*, 908–912, doi:10.2109/jcersj2.123.908.

69. Gao, Z.; Zhao, L. Effect of Nano-Fillers on the Thermal Conductivity of Epoxy Composites with Micro-Al2O3 Particles. *Mater. Des. 1980-2015* **2015**, *66*, 176–182, doi:10.1016/j.matdes.2014.10.052.

70. Pan, D.; Zhang, X.; Yang, G.; Shang, Y.; Su, F.; Hu, Q.; Patil, R.R.; Liu, H.; Liu, C.; Guo, Z. Thermally Conductive Anticorrosive Epoxy Nanocomposites with Tannic Acid-Modified Boron Nitride Nanosheets. *Ind. Eng. Chem. Res.* **2020**, *59*, 20371–20381, doi:10.1021/acs.iecr.0c04510.

71. Wang, X.; Zhang, X.; Bian, X.; Lu, C.; Li, Q.; Bai, C.; Zhang, L.; Zheng, T. Curing Kinetics and Mechanical Properties of an Underwater SiO_2 /Epoxy Adhesive. *J. Adhes.* **2023**, *99*, 1607–1625, doi:10.1080/00218464.2022.2151906.

72. Kumar, R.; Mishra, A.; Sahoo, S.; Panda, B.P.; Mohanty, S.; Nayak, S.K. Epoxy- based Composite Adhesives: Effect of Hybrid Fillers on Thermal Conductivity, Rheology, and Lap Shear Strength. *Polym. Adv. Technol.* **2019**, *30*, 1365–1374, doi:10.1002/pat.4569.

73. Han, S.; Meng, Q.; Pan, X.; Liu, T.; Zhang, S.; Wang, Y.; Haridy, S.; Araby, S. Synergistic Effect of Graphene and Carbon Nanotube on Lap Shear Strength and Electrical Conductivity of Epoxy Adhesives. *J. Appl. Polym. Sci.* **2019**, *136*, 48056, doi:10.1002/app.48056.

74. Jojibabu, P.; Jagannatham, M.; Haridoss, P.; Janaki Ram, G.D.; Deshpande, A.P.; Bakshi, S.R. Effect of Different Carbon Nano-Fillers on Rheological Properties and Lap Shear Strength of Epoxy Adhesive Joints. *Compos. Part Appl. Sci. Manuf.* **2016**, *82*, 53–64, doi:10.1016/j.compositesa.2015.12.003.

CURRICULUM VITAE

Name Surname: ESİN AKÇA

EDUCATION

Degree	Institution	Year of Graduation
MS	METU Metallurgical and Materials Engineering Department	2014
BS	METU Metallurgical and Materials Engineering Department	2011
High School	Bornova Anatolian High School	2006

WORK EXPERIENCE

ASELSAN / Manufacturing Directorate

- Manager — February 2026 – Present

ASELSAN / Microelectronic Device Design Department

- Team Lead — June 2024 – February 2026
- Design Engineer — December 2014– June 2024

IBM Almaden Research Center / Science and Technology Devision

- Visiting Researcher — June 2015 – February 2017

Yiğit Battery / R&D Department

- R&D Engineer — July 2011 – December 2014

METU / Metallurgical and Materials Engineering Department

- Project Researcher — July 2011 – December 2014

FOREIGN LANGUAGES

- English (Advanced)

PATENTS

- Thin cathode for micro-battery United States, Patent no: US11289704B2
  Mikro batarya için ince katot, 2018/04178, Rüçhan no: 15/629893
- Yüksek yüzey alanlı nano yapılara sahip metal malzeme için bir üretim yöntemi, 2018/00314

- Porous sheets United States, 2016 Patent no:US11005089B2
  Gözenekli tabakalar, 2017/11784, Rüçhan no: 15/243614

- Lityum-iyon bataryalarda kullanılan alaşımlı lityum mangan fosfat bileşiği ve bahsedilen bileşiğin üretim yöntemi, 2013/11711

- Lityum-iyon batarya malzemesinde yenilik, 2013/09189